In: Uranium: Characteristics, Occurrence and Human Exposure ISBN: 978-1-62081-207-5
Editors: Alik Ya. Vasiliev and Mikhail Sidorov

Chapter 4

LASER-INDUCED NUCLEAR DECAYS IN URANIUM ISOTOPES

G. A. Shafeev
Wave Research Center of A.M. Prokhorov
General Physics Institute of the Russian Academy of Sciences, Russia

ABSTRACT

Experimental results are reviewed on laser-induced accelerated nuclear decays in Uranium isotopes and nuclides of its branching under laser exposure of metallic nanoparticles in aqueous solutions of Uranium salts. Laser exposure of metallic targets (Au, Ag, Pd) in aqueous solutions of $^{238}UO_2Cl_2$ leads to generation of nanoparticles of corresponding materials in the bulk of the liquid and simultaneously shifts the secular equilibrium in the activity of nuclides of its branching, such as ^{234}Th and ^{234m}Pa. Real-time acquisitions of gamma-spectra of solutions indicate the presence of non-equilibrium gamma-activity in the range of photon energies between 50 and 60 keV. This activity is attributed to the laser-assisted generation of short-living isotopes ^{214}Pb and ^{214}Bi that stand at the end of ^{238}U branching. The experimental results are presented on laser-induced accelerated alpha-decay of ^{232}U under exposure of aqueous solution of its salt in presence of metallic nanoparticles. The results on the shift of secular equilibrium under laser action are compared with similar results on electro-explosion of metallic wires in aqueous solutions of Uranium salt. Possible mechanisms of laser-induced decays are discussed on the basis of amplification of the laser wave on metallic nanoparticles due to plasmon resonance.

INTRODUCTION

Since their advent more than 50 years ago lasers became versatile tools widely used both in variety of scientific researches and technological processes. Lasers produce a flow of highly organized photons, both in space and spectral range. This allows focusing laser beams to very small spatial dimensions that are, however, limited to the wavelength of laser light. The energy of laser photons is usually of several eV if no methods of frequency up-

conversion are used. Free electron laser systems are capable of generation of X-ray photons. Still, however, photon energies of laser photons are much smaller than characteristic energies of nuclear levels. Recent theoretical work shows the capability of laser radiation to directly excite nuclear levels of energy [1]. However, exciting a nuclear transition would require an x-ray or gamma-ray lasers with an intensity greater than 10^{20} Watts/cm^2.

At the same time, laser generated photons can indirectly influence the nuclear levels and alter or induce nuclear reactions. Laser beams at intensity level of 10^{18} W/cm^2 are capable of inducing nuclear transformations under laser exposure of solid targets in vacuum. This can be achieved at pico- and femtosecond laser pulse durations [2-4].

The emission of alpha-particles was observed under exposure of ^{11}B target to picosecond laser pulses. Experiments were carried out on the "Neodymium" laser facility at the pulse energy of 10–12 J and pulse duration of 1.5 ps. The composite targets $^{11}B + CH_{2n}$placed in vacuum were used. The yield of 10^3 alpha particles per pulse has been detected at peak laser intensity on the target of 2×10^{18}W/cm^2 [5]. The mechanism of initiation of a neutron-less fusion reaction is due to the acceleration of electrons and protons in the plasma separated by strong laser field.

Another approach to laser initiation of nuclear reactions is based on the laser exposure of nanoparticles suspended in a liquid (colloidal solution). This process becomes possible at much lower level of intensities of laser radiation in the medium, of order of 10^{12}-10^{13} W/cm^2. The crucial role in laser-induced acceleration of nuclear decays belongs to nanoparticles (NPs) that interact with laser beam in presence of unstable isotopes. Each nanoparticle can be considered as a target for laser exposure. Unlike bulk targets, metal nanoparticles are optically thin. The critical density is reached from the onset of laser pulse; this is the density of free electrons in the nanoparticle but owing to the small size of the target the reflection is negligible. In this case the whole nanoparticle is heated up by the laser beam homogeneously. The same applies to the late stages of laser heating – the material of the target is ionized and expands in the shape of spherical cavity but the laser radiation is still absorbed by the plasma due to the small size of the cavity. Small size of NPs leads to local enhancement of the field of laser wave, and the efficient intensity in the vicinity of nanoparticle can be several orders of magnitude higher due to plasmon resonance of charge carriers. Such electric field is already comparable with electric fields inside the atoms and this causes significant distortion of electronic shells. This distortion, in turn, alters the probability of spontaneous nuclear decays, either alpha- or beta ones.

Since the acceleration of nuclear decays occurs under exposure of a solid target immersed into liquid to laser radiation, an introduction section is needed to outline main phenomena that take place in this experimental setup.

GENERATION OF NANOPARTICLES UNDER LASER ABLATION OF SOLIDS IN LIQUIDS

Formation of nanoparticles under laser ablation of solids either in gas or in vacuum has been extensively explored during the last decade. Understanding of the mechanisms of cluster formation is needed to control the process of Pulsed Laser Deposition (PLD) that is widely used now for deposition of a large variety of compounds. Formation of nanoparticles under

laser ablation of solids in liquid environment has been studied to a lower extent. A number of wet chemical methods of nanoparticles (NPs) preparation are known up to date. Laser ablation of solids in liquid environment emerged as an alternative technique that is capable of producing "pure" NPs without counter-ions and surface-active substances. Primary motivation for generation of NPs by laser exposure of solid targets in liquids was the hope that pure NPs would be more efficient in the process of Surface Enhanced Raman Scattering (SERS), since no other compounds can obscure the surface of metallic NPs [6-10].

Formation of both large varieties of NPs under laser ablation of corresponding solids has been reported during the last decade [11-23].

Further studies showed that the laser ablation in liquids is a complex process with a number of experimental parameters. In particular, interaction of ejected nano-sized species with hot liquid vapors at high transient pressure results in large diversity of final particles that remain in the liquid. Also, surface tension at the interfaces is dominant force that governs the dynamics of interaction of molten target material with vapors of surrounding liquid on a nanometer scale. Under pulsed laser exposure the liquid also undergoes chemical changes that may be stipulated by ejected NPs that act in this case as a catalyst. Initially liquid substance may become supercritical in the vicinity of the target, which alters its reactivity and opens new channels of chemical reactions especially in case of aqueous solutions.

Interaction of metal nanoparticles with laser light proceeds via its absorption by free electrons. Free electrons exhibit plasmon resonance, whose position is determined by both their concentration, their effective mass (that depends on the solid) and particle size. NPs of noble metals, e.g., Au or Ag, show a strong selective absorption in the visible, so the suspensions of these NPs in liquids are colored. Plasmon resonances of other metallic NPs are situated in the UV region. Though if the liquid is transparent at the onset of laser exposure of the target, the appearance of NPs may change this situation, and the laser radiation is absorbed by the colloidal solution. This may lead to poor control of the laser spot size on the target due to either thermal lensing inside the solution or different non-linear phenomena induced by laser beam in NPs. The position of plasmon resonance of metallic NPs virtually coincides with that of NS generated on bulk targets under their laser ablation in liquids (see above). In other words, metallic NPs in the bulk of the solution are of the same origin as NS left after solidification of the melt on the target. These NPs represent the part of the target material that has been sputtered into the liquid under the action of the pressure wave of the liquid that surrounds the target. The well-studied NPs generated by laser ablation in liquids are gold NPs. This is due to their perfect chemical stability, which guarantees the metallic nature of generated NPs. Synthesis of a stable colloidal solution of Au NPs in water has been reported by several groups [31 – 35].

Optical and chemical properties of Au NPs are thoroughly explored owing to well-established chemical methods of their synthesis. Spherical Au NPs are characterized by a single (degenerated) band of plasmon resonance situated in the visible range of spectrum. Elongated Au NPs are characterized by two plasmon bands situated in the visible, and their position varies with the aspect ratio of NPs. This offers a good coupling of the visible laser radiation to Au NPs. Moreover, tuning the laser wavelength in various parts of their spectrum allows shape-selective fragmentation of Au NPs [36].

Typical view of Au NPs generated by the laser exposure of a bulk Au target in water radiation of a Cu vapor laser in D_2O is presented in Figure 1.

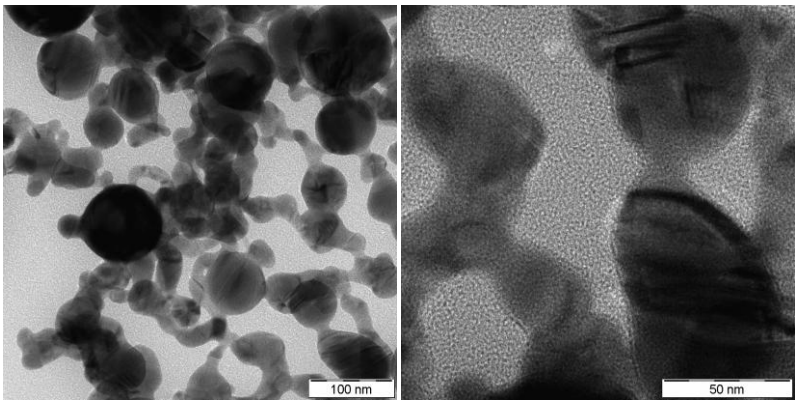

Figure 1. Transmission Electron Microscope (TEM) view of Au NPs generated by ablation of Au NPs in D_2O by radiation of a Cu vapor laser, wavelength of 510 nm, pulse duration of 15 ns.

Average size of generated NPs is about 50 nm and in general depends on the laser fluence on the target. Generated NPs remain in the solution and can be again exposed to the laser beam. This secondary exposure of NPs causes the change of their average size, and the size distribution function of NPs shifts to lower dimensions. This is so called fragmentation process. Fragmentation of NPs under their laser exposure in liquids has been reported as early as the synthesis of NPs itself [6, 11, 19]. The process manifests itself as a gradual decrease of the size of NPs upon laser irradiation. As a result, the distribution function of particle size shifts to lower dimensions. Optical constants of metallic targets do not vary largely in the wavelength range of lasers used for NPs synthesis, so fragmentation of NPs should be ascribed to interaction of synthesized NPs themselves with the laser beam inside the liquid.

The physical processes that lead to fragmentation of NPs in the laser beam are still under discussion. The most probable reason leading to reduction of NPs size are the instabilities that develop at the interface of molten NPs with the vapors of surrounding liquid [24]. Indeed, NPs may absorb enough energy from the laser beam to undergo the phase transition into a liquid state. The temperature of NPs exceeds at this moment the boiling temperature of surrounding liquid. The latter is therefore vaporized and forms a shell around the NPs. The pressure of vapors in this shell is around 10^8 Pa, and its possible asymmetry would result in the break of molten NPs inside it into smaller parts. The most probable process is splitting of the molten NPs into two equal particles, since, first, this corresponds to lowest value of total surface energy, and second, is the lowest mode of perturbation of the surface of molten NPs. This hypothesis is in qualitative agreement with the fact that the average size of NPs exposed to laser radiation in various liquids decreases with the decrease of boiling temperature of the liquid. The balance is gained when the pressure inside the NPs of radius R is of order of the pressure of the surrounding liquid p_{liq}: $2\sigma/R \sim p_{liq}$, where σ stands for the surface tension of molten NPs.

Fragmentation of the NPs under their laser exposure introduces feedbacks into the system "laser radiation – NPs". Indeed, the average size of NPs under their laser exposure is inversely proportional to the peak intensity of the laser beam inside the liquid. The size of NPs decreases upon exposure till they become so small that the energy absorbed from the laser pulse is not sufficient for melting. The system therefore demonstrates a negative feedback and auto-stabilization. On the other hand, melting temperature of NPs decreases

with its size, which is a positive feedback. Finally, small NPs formed via fragmentation from bigger ones do not absorb enough energy from the laser beam to be molten, and the ensemble of NPs acquires its lower limit of their size.

NANO-STRUCTURES FORMATION UNDER LASER EXPOSURE IN LIQUIDS

Laser exposure of a metallic target in liquid environment leads not only to ejection of NPs into the surrounding liquid. The rate of NP generation depends not only on the laser fluence, but also of experimental parameters such as the metal reflectivity at the laser wavelength, the nature of the liquid, etc. The rate of NP production decreases with the laser fluence. At lower fluence the rate of NP generation drops, while the surface of the target undergoes eye-visible changes. The coloration of the exposed areas is well pronounced while the target remains in the liquid, whereas it fades if the target is removed from the liquid and dried. In case of the Ag target the color of laser-treated areas is yellow, though the maximum of absorption for freshly-exposed Ag surface lies in UV region (370 nm, [25]). Exposed areas of Au sample look like metallic copper with corresponding maximum of absorption around 570 – 590 nm. The coloration is due to plasmon oscillations of free electrons in nano-protrusions of the surface exposed to laser radiation in water.

The formation of nanostructures on a rough metal surface subjected to laser ablation in water is due to the modification of the topology of the molten area upon decreasing the laser fluence. At high laser fluence (~ 1 J/cm^2 in our case), the molten area is continuous, and this melt is effectively dispersed as nanoparticles by the recoil pressure of the surrounding liquid. The recoil pressure of the vapor surrounding the target pushes these molten areas from the target and generates a nano-relief.

In other words, formation of nano-spikes is a result of a hydrodynamic instability at the interface “liquid vapor – melt” characterized by very small period of order of hundreds of nanometers. The described mechanism is independent on the target material, and similar nanostructures may be grown on any other material that absorb at the laser wavelength.

These data are corroborated with the images taken with a. The surface of either Ag or Au target is covered by a dense array of nanostructures (Figure 2). Of course, the protruding NS will be molten by the next laser pulse since they weak thermal coupling with the substrate. However, new NS will arise as soon as the laser pulse is over, and each subsequent pulse will be absorbed by nano-structured surface of the target. Therefore, interaction of pulsed laser radiation with metals immersed into liquid is characterized by formation of different nano-objects: nanoparticles in the liquid and nanostructures left on the target surface. The technique of laser ablation in liquids is very flexible and allows generating NPs of numerous metals and compounds in virtually any liquid. New phenomena arise if metallic NPs are dispersed in the aqueous solution of salts of unstable isotopes, e.g., Uranium. Laser exposure of such solution leads to irreversible changes of its activity and activities of its daughter nuclides. As it is demonstrated below, laser exposure accelerates both alpha- and beta-decays of all nuclides of ^{238}U branching. The effect of laser exposure of NPs on the activity on unstable isotopes was firstly observed in aqueous solutions of ^{232}Th salts [26].

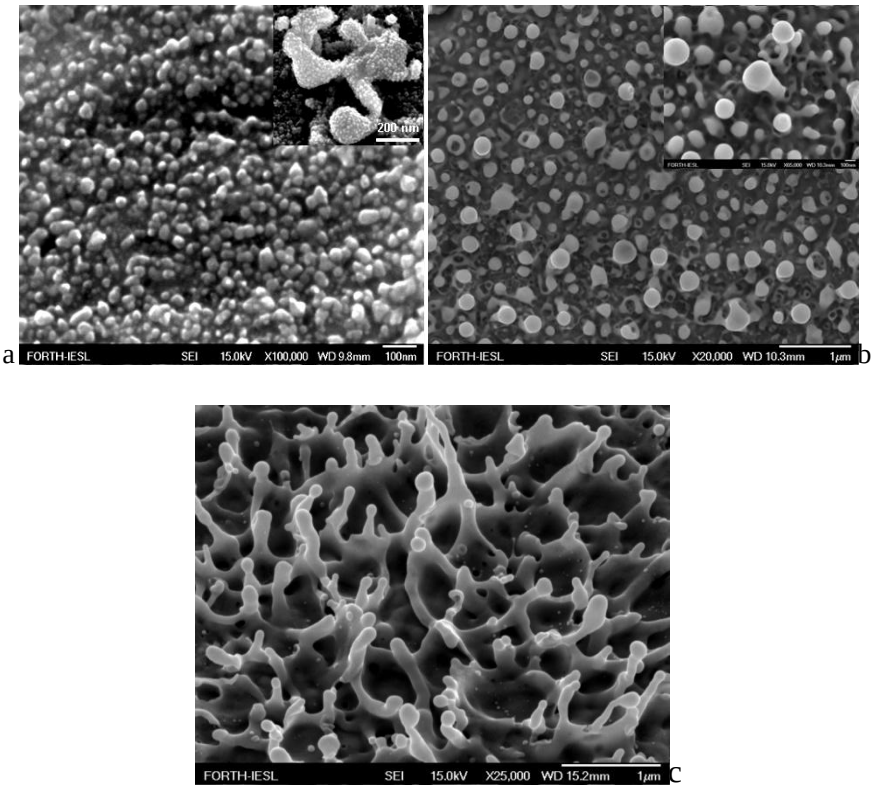

Figure 2. Scanning Electron Microscope with Field Emission (FE SEM) view of NS on Ag (a) and Au (b) targets produced by their ablation in water with radiation of a 5 psKrF laser, wavelength of 248 nm. Insets show the view at different scale. NS on bulk Au produced by femtosecond laser exposure in water, wavelength of 800 nm, pulse duration of 100 femtosecond (c).

It was experimentally found that the activity of daughter nuclides can be affected by laser exposure of Au NPs in solutions of $Th(NO_3)_4$. Also, laser exposure altered the activity of ^{137}Cs presented in the solutions as impurity. Further investigations showed that this phenomenon is rather general and is also observed in solutions of Uranium salts subjected to laser pulses of high intensity of order of 10^{12} W/cm^2, though this intensity is several orders of magnitude smaller than used in above mentioned experiments on laser exposure of various targets in vacuum.

The results of laser-induced accelerated decay of Uranium isotopes are compared with experimental results obtained as early as in 2002 on deviation of secular equilibrium in Uranium nuclides under electro-explosion of metallic foils in aqueous solutions of Uranil.

AQUEOUS SOLUTIONS OF URANIL-IONS

Aqueous solutions of Uranil salts of natural isotope composition were used in all experiments, either $UO_2(NO_3)_2$ or UO_2Cl_2. Both salts dissociate in aqueous medium to UO_2^{-2} ion and corresponding anion. Uranium demonstrates 6+ valency in these compounds. In order to affect the activity of nuclides, the laser radiation should becoupled to the solution. This can

be achieved using metallic nanoparticles suspended in the solution of Uranium salt. Figure 3 shows absorption spectra of both colloidal solutions of Au NPs and aqueous solutions of UO_2Cl_2. Radiation of both Cu vapor laser and the second harmonics of a Nd:YAG laser is efficiently absorbed by Au NPs owing to plasmon resonance of electrons in NPs situated for Au around 530 nm.

The absorption of the solution increases in UV range of spectrum, and the radiation of the third harmonics of a Nd:YAG laser with wavelength of 355 nm is strongly absorbed by Au NPs due to inter-band transitions. Moreover, this radiation is absorbed by Uranil-ion itself causing its strong green luminescence.

The fundamental output of a Nd:YAG laser at wavelength of 1064 nm lies outside the absorption range of the above solution. However, under sufficiently high intensity of laser radiation NPs serve as centers for ionization, and laser radiation couples to the colloidal solution through absorption by plasma shells around NPs. The density of electrons in these shells varies during the laser pulse but at each moment before recombination of plasma they can be considered as nanoparticles of plasma that are characterized with their own plasmon resonance.

That is why as it will be demonstrated below the influence of laser exposure on the activity of radionuclides in the solution weakly depends on the nature of NPs. The initial absorption due to plasmon resonance of electrons in specific metallic NPs serves as a precursor for further development of plasma cloud around NPs.

The decay of ^{238}U proceeds through well known sequence of alpha- and beta-decays of these isotopes and their daughter nuclides:

$$^{238}U \rightarrow {}^{234}Th \rightarrow {}^{234m}Pa \rightarrow {}^{234}U \rightarrow \ldots {}^{214}Pb$$

Typically, beta-decay leads to the formation of daughter nuclei in the excited state, and gamma-emission of this daughter nuclide allows tracing its activity.

In the equilibrium conditions (so called secular equilibrium) the ratio of activities of neighboring nuclides is inversely proportional to their half-life times.

This equilibrium ratio shifts under laser exposure of metallic NPs in aqueous solution of salts of Uranium. As it will be seen from results presented below the deviation from secular equilibrium is observed for both isotopes ^{238}U and ^{235}U and their daughter nuclides. High isotope selectivity is observed in certain range of laser parameters.

Namely, the activity of ^{238}U branching is strongly affected by laser exposure of the solution, while the activity of ^{235}U in the same solution remains constant within the accuracy of measurements. Similar results were experimentally studied for another Uranium isotope, namely, ^{232}U. The influence of laser exposure on the activity of nuclides of ^{238}U branching was estimated on the basis of gamma-spectra of solutions before and after exposure. Typical gamma-spectrum of the solution of UO_2Cl_2 used in the work is presented in Figure 4. The emission of gamma-photons accompanies the beta-decay of corresponding nuclides.

The activities of isotopes ^{234}Th, ^{234m}Pa, and ^{235}U before and after laser exposure were measured in the following series of experiments. The gamma-activity of ^{235}U was determined form the gamma-activity of its daughter nuclide ^{231}Th [27]. The activity was calculated as the area under the corresponding peaks of gamma-spectrum.

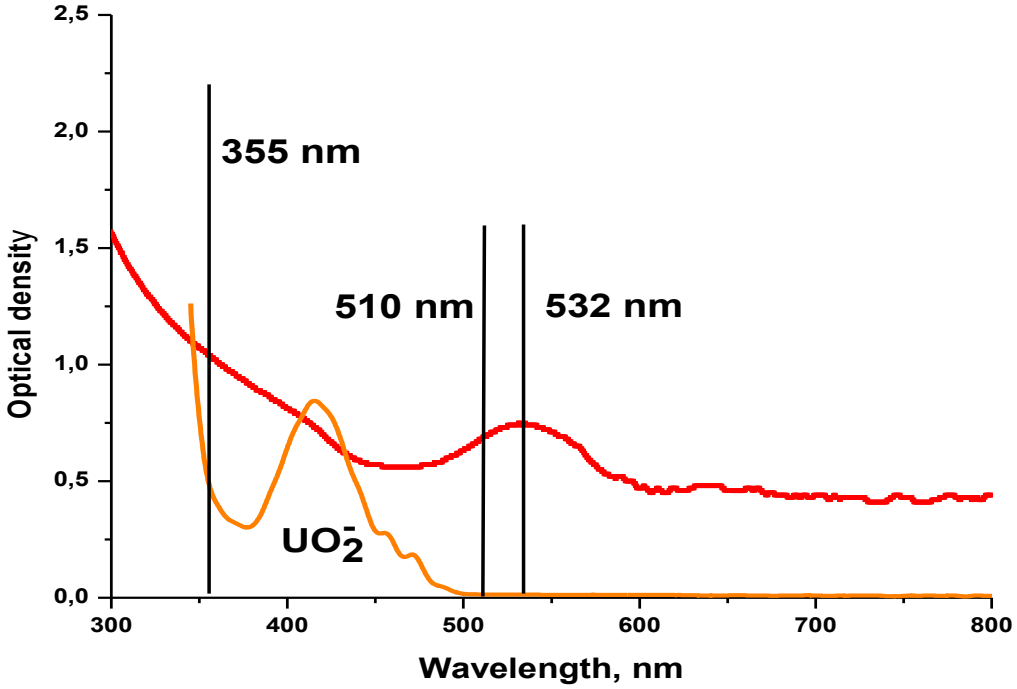

Figure 3. Absorption spectra of an aqueous solution of UO_2Cl_2 (orange) and of a colloidal solution of Au NPs (red). Vertical lines indicate the position of the second and third harmonics of a Nd:YAG laser as well as the position of the emission line of a Cu vapor laser. The position of the first harmonics of a Nd:YAG laser at 1064 nm is not shown.

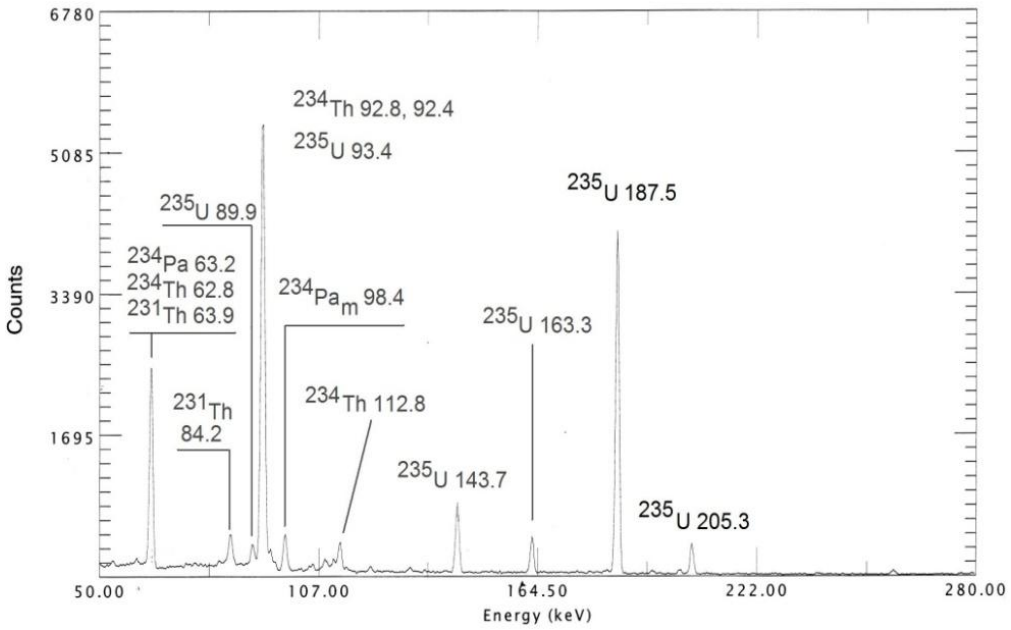

Figure 4. Gamma-spectrum of the initial solution of UO_2Cl_2 in H_2O. The spectrum obtained with the help of a semiconductor gamma-spectrometer Ortec-65195-P.

LASER EXPOSURE OF AQUEOUS SOLUTIONS OF URANIL-CHLORIDE WITH AU NANOPARTICLES

Gold is the most stable metal against oxidation, which stipulates its frequent use for laser generation of NPs. Colloids of Au NPs in pure water are perfectly stable without addition of any surface active substances. First experiments with laser-induced nuclear decays have been conducted exposing the mixture of colloidal solutions of Au NPs generated by laser ablation of a bulk Au target with aqueous solutions of UO_2Cl_2.

However, the presence of Cl^- ions in the solution leads to rapid sedimentation of Au NPs. The NPs agglomerate and sediment on the cell walls. Therefore, the absorption of laser radiation in the medium decreases with time and its coupling becomes less efficient. New approach has been elaborated to overcome this problem.

Namely, the solution of Uranium salt initially does not contain NPs. Instead, a bulk Au target is placed inside the solution, and NPs are generated by laser ablation of this target by laser beam focused through the layer of solution. In this way NPs are generated during laser exposure of the solution, and their concentration varies during exposure. In this case the presence of anions is not that critical for the stability of the colloid. Indeed, if NPs agglomerate, new NPs are generated at their place. This approach is schematically illustrated in Figure 5.

One more advantage of this scheme is the generation of nanostructures (NS) on the target surface, which is especially pronounced under ablation of metal using sub-nanosecond laser pulses.

These NS may contribute to the amplification of the laser wave in their vicinity. The temperature rise in the cell during laser exposure depends on the average power of laser radiation and in typical conditions does not exceed 10 K. At higher average power of laser radiation of several Watts cooling of the cell with water flow can be used. The following sections describe the results of laser exposure of Au target in aqueous solutions of UO_2Cl_2 to different laser sources [28].

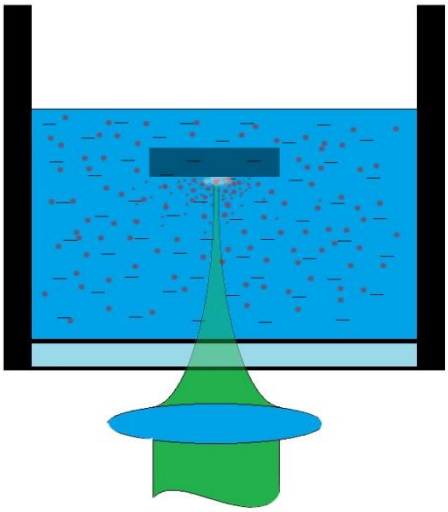

Figure 5. The scheme of laser exposure of metallic target in aqueous solution of Uranil-chloride.

FEMTOSECOND TI: SAPPHIRE LASER

Laser exposure of the target has a pronounced effect on the activity of the nuclides present in the solution. Changes occur at all the gamma photon energies characteristic of a given nuclide. As an example, Figure 6 illustrates the effect of laser exposure on the ^{234}Th activity. The activity is seen to markedly decrease. At the same time, it depends little on whether the exposure was performed in heavy or light water. The half-life of ^{234}Th is 24 days, so its activity just after the exposure was even lower than that in Figure 6.

Figure 7 illustrates the influence of laser exposure on the activity of the nuclides in question. After the laser exposure, the activity was measured twice, which allowed us to examine its relaxation to the equilibrium state. The activities of the three nuclides are seen to decrease.

After the exposure, the ^{234}Th and ^{234m}Pa activities gradually approach their initial level, whereas the ^{235}U activity varies insignificantly. This is due to the continuing spontaneous alpha decay of ^{238}U to ^{234}Th and then to ^{234m}Pa. Note that the above data qualitatively correlate with results for aqueous uranium salt solutions exposed to 150-ps 1064-nm Nd : YAG pulses [29].

When there are no external influences, each nuclide of the ^{238}U series has an equilibrium activity, determined by its half-life. ^{235}U belongs to another decay series and, when alpha-decaying to ^{231}Th, it has an equilibrium activity. The ^{234}Th to ^{235}U activity ratio in uranium of natural isotopic composition is constant under secular equilibrium conditions. The A_{234Th}/A_{235U} activity ratio in solutions after 800-nm femtosecond laser exposure is presented in Figure 8.

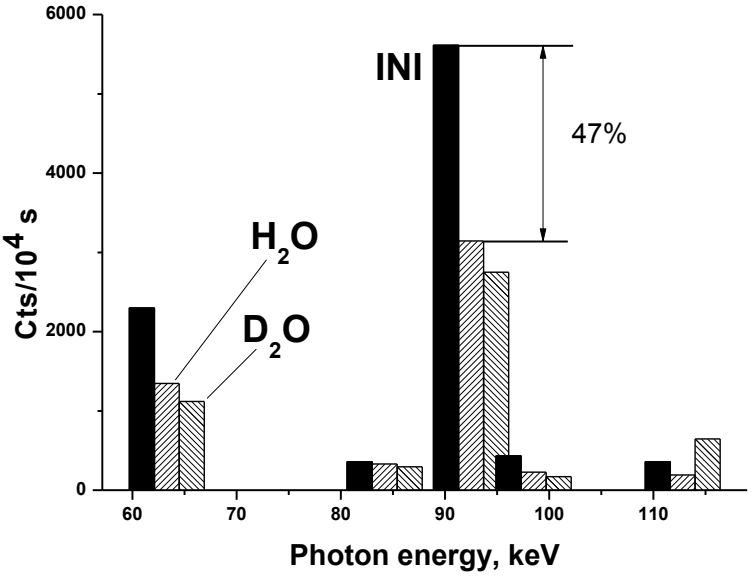

Figure 6. Activity of Thorium-234 before (INI) and after laser exposure of solutions of UO_2Cl_2 in H_2O и D_2O. Laser wavelength of 800 nm, pulse duration of 180 fs. Exposure time of 1 hour at repetition rate of laser pulses of 1 kHz. Gamma-spectra were acquired 14 days after laser exposure, accuracy of activity measurements is ±5%.

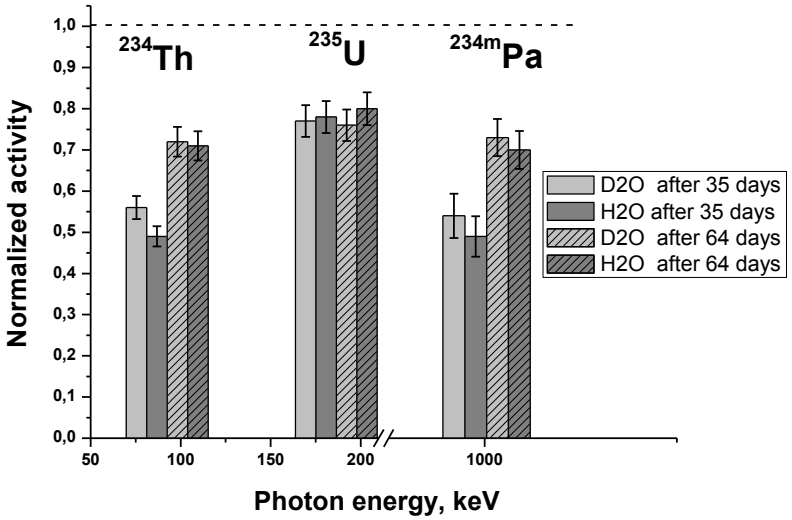

Figure 7. Activities of ^{234}Th (92.5 keV), ^{235}U (186.5 keV), and ^{234m}Pa (1001 keV) normalized on their activity in the initial samples. The activities of laser-exposed samples either in H_2O or in D_2O were measured 35 and 64 days after laser exposure. Dashed line denotes the ratio of activities in the initial sample. Ti:sapphire laser, wavelength of 800 nm, pulse duration of 180 fs. Exposure during 1 hour at repetition rate of 1 kHz.

Laser exposure of solutions results in the decrease of activities of all of three nuclides. The activities of both ^{234}Th and ^{234m}Pa recover to their initial value with time after laser exposure. This is due to the continuing alpha-decay of ^{238}U to ^{234}Th, which in turn decays to ^{234m}Pa. Note that the activity of ^{235}U does not change after laser exposure and remains constant within the accuracy of measurements being still smaller than in the initial sample. This behavior is evident since there is no parent nuclide for ^{235}U.

In the conditions of secular equilibrium the activity of all nuclides of ^{238}U branching has its equilibrium value. ^{235}U belongs to another branching, and its activity also has its equilibrium value that is established during its alpha-decay to ^{231}Th. The ratio of activities of ^{234}Th and ^{235}U in Uranium of natural isotopic composition is constant in secular equilibrium. Deviation of this ratio from its equilibrium implies the presence of non-equilibrium processes induced by laser radiation in respective branches. The ratio of activities of ^{234}Th and ^{235}U after exposure of Au target in either H_2O or D_2O to femtosecond laser radiation is plotted in Figure 8. One can see that the activity ratio undergoes strong changes after laser exposure and then recovers to its initial equilibrium value.

Since the variation activity of ^{235}U after laser exposure is relatively small, one may ascribe the restoration of the activity ratio to recovery of the activity of ^{234}Th. The activity ratio of Thorium-234 and Uranium-235 in the initial sample was measured twice. One can see that this value is the same in these two independent measurements. This confirms the reliability of measurements.

Laser exposure markedly reduces this ratio, which then gradually reverts back to its initial level. The deviation of the activity ratio from its equilibrium value is essentially independent of water composition (H_2O or D_2O). Similar deviation of the activity ratio of these nuclides is observed under electro-explosion of Ti foils in Uranil solutions (see corresponding section below).

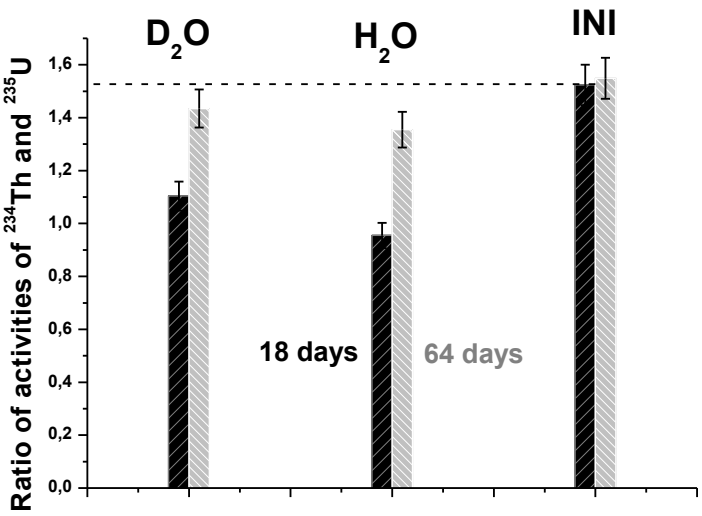

Figure 8. Ratio of activities of Thorium-234 and Uranium-235 measured at 92.5 and 185 keV, respectively, under exposure of a bulk Au target in aqueous solutions of Uranil-chloride to femtosecond laser radiation. Measurements were carried out 18 (black columns) and 64 days (light columns) after laser exposure. Dashed line shows the activities ratio in the initial sample.

PICOSECOND ND: YAG LASER

Nd:YAG lasers are currently the most popular laser sources. Frequency up-conversion using non-linear crystals allows covering wide spectral range. In particular, frequency up-conversion of the fundamental output at 1064 nm of these lasers may couple radiation to different parts of absorption spectra of Au NPs and Uranil ion (see Figure 3) [30]. Initiation of nuclear decays using the first harmonics of a picosecond Nd:YAG laser is presented in details elsewhere [29]. Experimental results on laser initiation of decays in Uranium branching under exposure to harmonics of a Nd:YAG laser are presented in this section.

SECOND HARMONICS (532 NM)

The exposure of a gold target to the second harmonic, which lies within the plasmon resonance of gold nanoparticles, in aqueous Uranyl-chloride solutions is also accompanied by a considerable deviation of nuclide activities from their equilibrium values. Figure 9 plots the activities of the three main nuclides in irradiated solutions against UO_2Cl_2 concentration. As seen, the ^{234}Th and ^{234m}Pa activities in the irradiated solutions markedly exceed those in the non-exposed solution, and the deviation of the activities increases with increasing concentration.

At the same time, the ^{235}U activity in the same irradiated solutions coincides with its equilibrium value to within the present measurement accuracy. This means the efficient enrichment of the solution by ^{235}U isotope. One can see from the plots above that the activities of both ^{234}Th and ^{234m}Pa are much higher than that in non-exposed solutions, and this deviation increases with concentration of UO_2Cl_2.

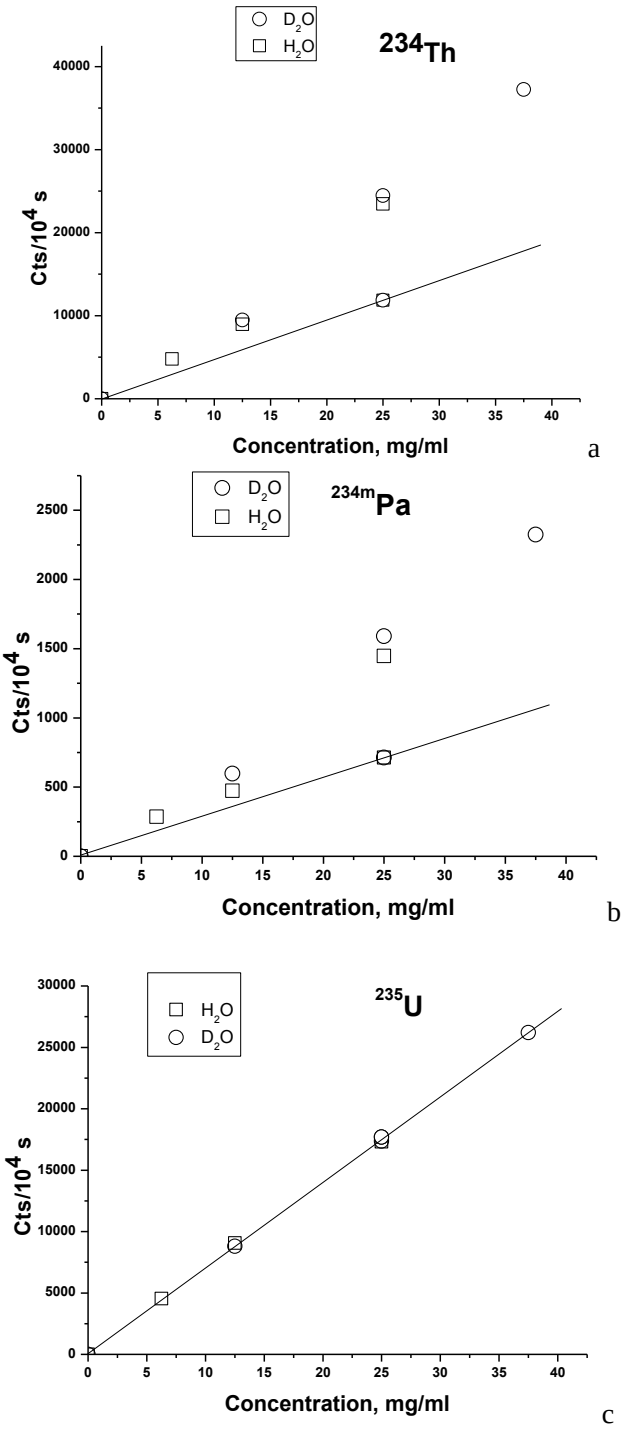

Figure 9. (a) ^{234}Th, (b) ^{234m}Pa, and (c) ^{235}U activities (counts over acquisition time of 10^4 s) as functions of concentration for Uranyl-chloride solutions in D_2O (circles) and H_2O (squares) containing gold nanoparticles and exposed to the second harmonic of a neodymium laser at 532 nm and pulse duration of 150 ps. The straight lines are drawn through the nuclide activities before the exposure. The size of the symbols represents the experimental error.

At the same time, the activity of ^{235}U in the same exposed probes remains at its equilibrium values. Therefore, very high isotopic selectivity is observed under exposure of a bulk Au target in aqueous solutions of UO_2Cl_2 to picosecond radiation at wavelength of 532 nm. The increase of activity of Thorium-234 indicates accelerated alpha-decay of its parent nuclide Uranium-238. In turn, the increase of activity of Protactinium-234m indicates that Thorium-234 undergoes accelerated beta-decay.

This observation is in good agreement with results of previous studies on electro-explosion of metallic wires in aqueous solutions of Uranil salts, as will be described in the corresponding section below.

THIRD HARMONICS (355 NM)

UV laser exposure of a gold target in an aqueous Uranyl-chloride solution at pulse duration of 150 ps leads to a considerable deviation of the A_{234Th} /A_{235U} ratio from its equilibrium value and in some range of parameters this deviations reaches a 5-fold decrease. This activity ratio is shown in Figure 10 as a function of uranium salt concentration in solution.

Laser exposure markedly reduces the ^{234}Th activity, whereas the ^{235}U activity changes little. That the activity ratio approaches its equilibrium value at high Uranium salt concentrations seems to be caused by the fact that the solution absorbs the laser radiation while it travels towards the target. As a result, the rate of gold nanoparticle generation decreases with increasing salt concentration, and laser exposure has a weaker effect on the nuclide activities.

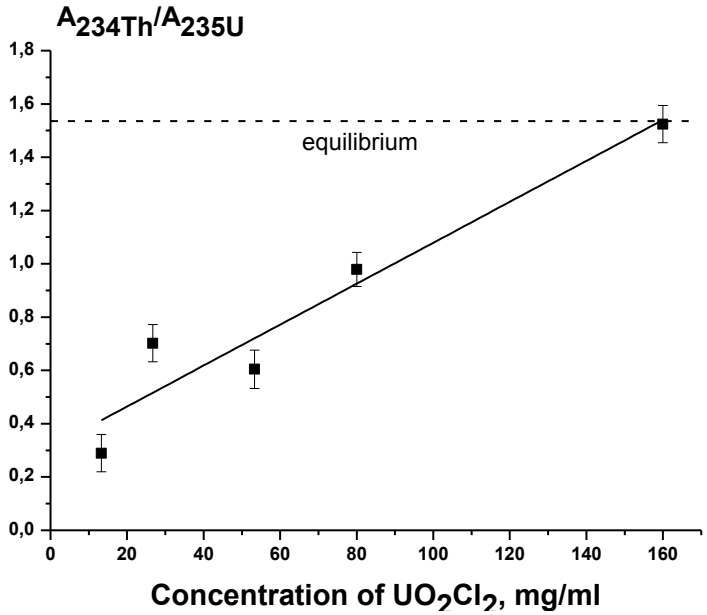

Figure 10. $^{234}Th/^{235}U$ activity ratio as a function of UO_2Cl_2 concentration in D_2O after 36 000 pulses of the third harmonics of a Nd:YAG laser at wavelength of 355 nm and pulse duration of 150 ps. The dashed line shows the equilibrium activity ratio.

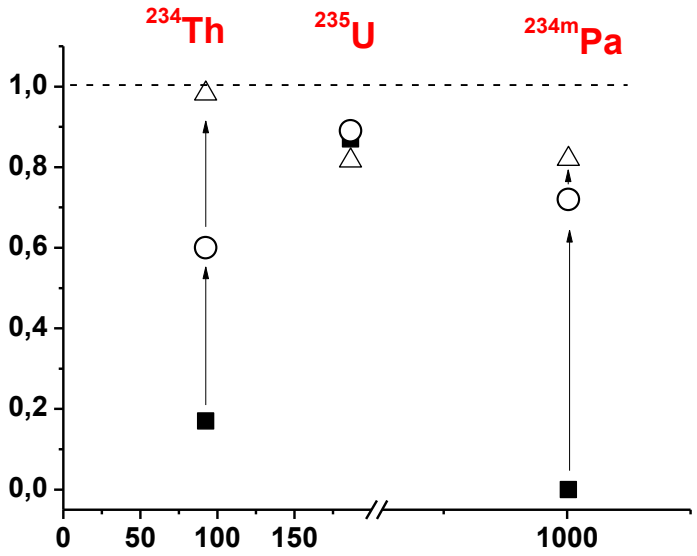

Figure 11. Normalised ^{234}Th (92.5 keV), ^{235}U (186.5 keV) and ^{234m}Pa (1001 keV) activities after laser exposure of a gold target. The activities are normalized to their values before the exposure. The measurements were made 28 (solid squares), 66 (open circles) and 131 days (open triangles) after laser exposure (36 000 pulses) in H_2O at the Uranyl-chloride concentration of 13.3 mg/mL. The dashed line indicates the activity before the exposure. The vertical arrows show the change in activity between the measurements. The size of the symbols represents the experimental error.

Figure 11 shows normalized activities of the three nuclides in irradiated solutions at the lowest salt concentration. As in the case of 800-nm Ti:sapphire laser exposure, the Nd : YAG third harmonic reduces the nuclide activities, including that of ^{235}U. The ^{234m}Pa activity 77in the irradiated sample was zero to within the present experimental uncertainty. It reached a measurable level only two months after the laser exposure. Moreover, the gamma spectra of irradiated samples contained peaks of nuclides (e.g. ^{214}Pb) that had not been detected in the solution before the laser exposure.

One can see that the activity of ^{234m}Pa is 0 within the accuracy of gamma-measurements even 28 days after laser exposure. Here again, the activity of ^{235}U remains constant after laser exposure being slightly lower than that in the initial sample. This means very large drop of activities ratio of ^{234}Th and ^{235}U induced by laser exposure and indicates large deviation from secular equilibrium.

LASER EXPOSURE OF URANIL-CHLORIDE SOLUTIONS WITH NPS OF PALLADIUM

In another series of experiments the influence of laser exposure on the activity of radio-nuclides was tested using NPs of Pd dispersed in the solution of Uranil-chloride [30]. The plasmon resonance of Pd NPs lies in UV range near 250 nm. The position of this resonance is red-shifted with the increase of NPs size making them suitable for coupling UV laser radiation to the solution.

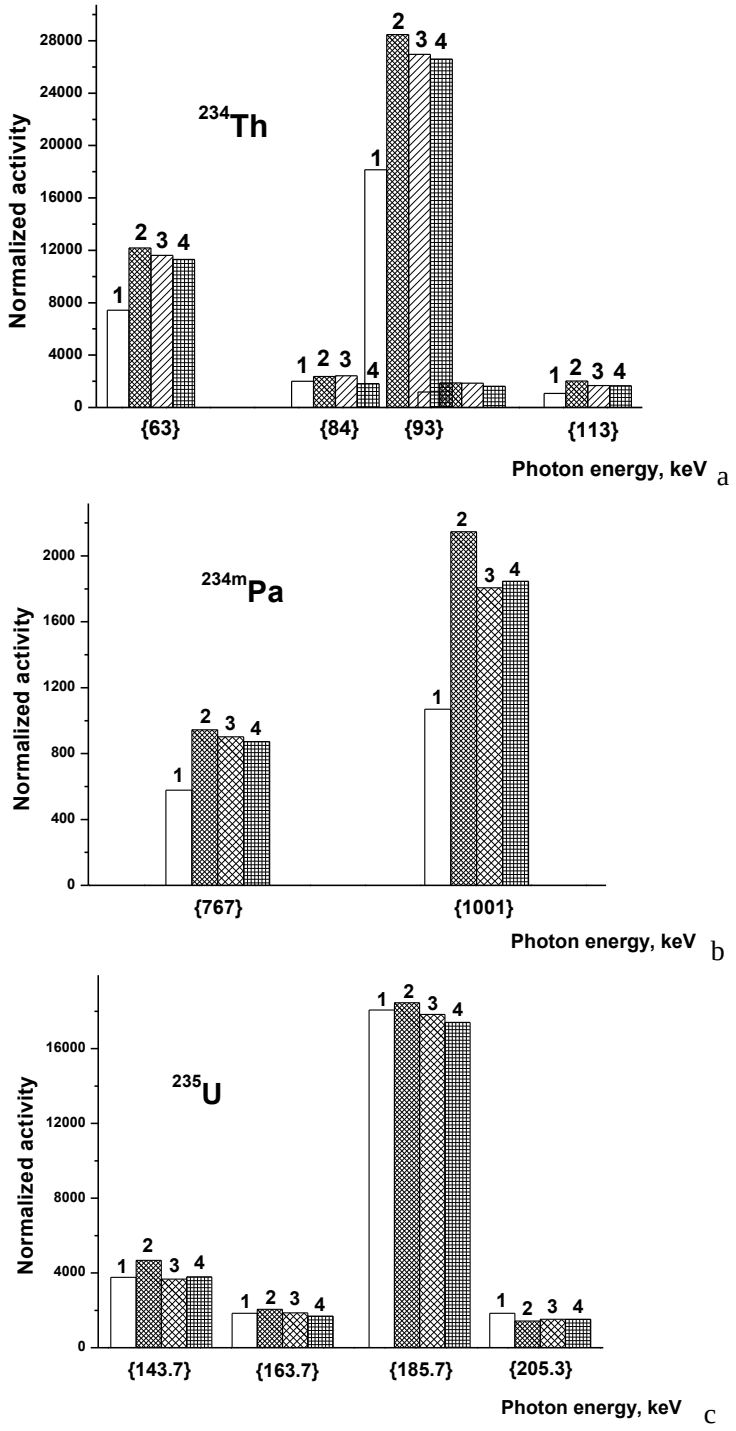

Figure 12. Normalized activities of ^{234}Th (a), ^{234m}Pa (b), and ^{235}U (c) after laser exposure of aqueous solutions of UO_2Cl_2 with Pd NPs. Changes of activities are shown on main photon energies of each nuclide. Laser wavelength of 355 nm, pulse duration of 150 ps, 1 hour exposure at repetition rate of 10 Hz. Concentration of UO_2Cl_2: 1 (initial solution) – 93 (in H_2O), 2 – 47 (in H_2O), 3 – 47 (in H_2O), 4- 23 (in D_2O) mM. Estimated peak power in the solution of 10^{11} W/cm^2.

Pd NPs were generated by ablation of a bulk Pd target in either H_2O or D_2O. Laser exposure of UO_2Cl_2 solutions with Pd NPs was carried out using the same scheme as for Au NPs. Third harmonics of a Nd:YAG laser was used at wavelength of 355 nm and pulse duration of 150 ps. Comparison of nuclides activities before and after laser exposure is presented in Figure 12.

Changes of nuclide activities are symbatical for all energies of gamma-photons of the same nuclide. The activity of ^{234}Th increases after laser exposure, which can be explained by accelerated alpha-decay of its parent nuclide ^{238}U. The activity of ^{234m}Pa changes in a similar way. On the contrary, the activity of ^{235}U after laser exposure remains the same within the accuracy of measurements, similarly to results obtained with Au NPs. Note that the deviation of nuclide activities is not sensitive to the type of aqueous medium.

LASER EXPOSURE OF URANIL-CHLORIDE SOLUTIONS WITH AG NPS

Next series of experiments dealt with laser exposure of aqueous solution of Uranil-chloride in presence of Ag NPs. Plasmon resonance of Ag NPs in water is centered at 400 nm, as shown in Figure 13.

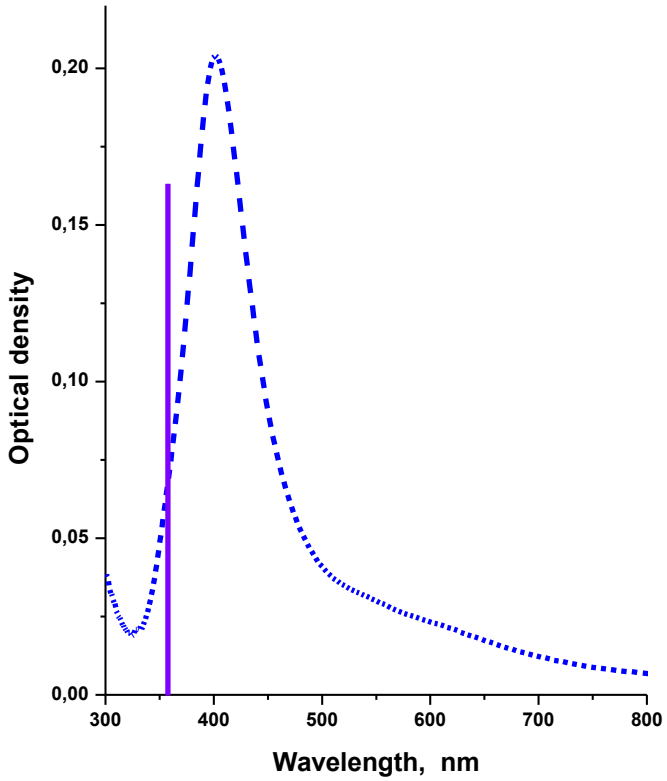

Figure 13. Absorption spectrum of Ag NPs in water. Vertical line indicates the position of the third harmonics of a Nd:YAG laser at 355 nm.

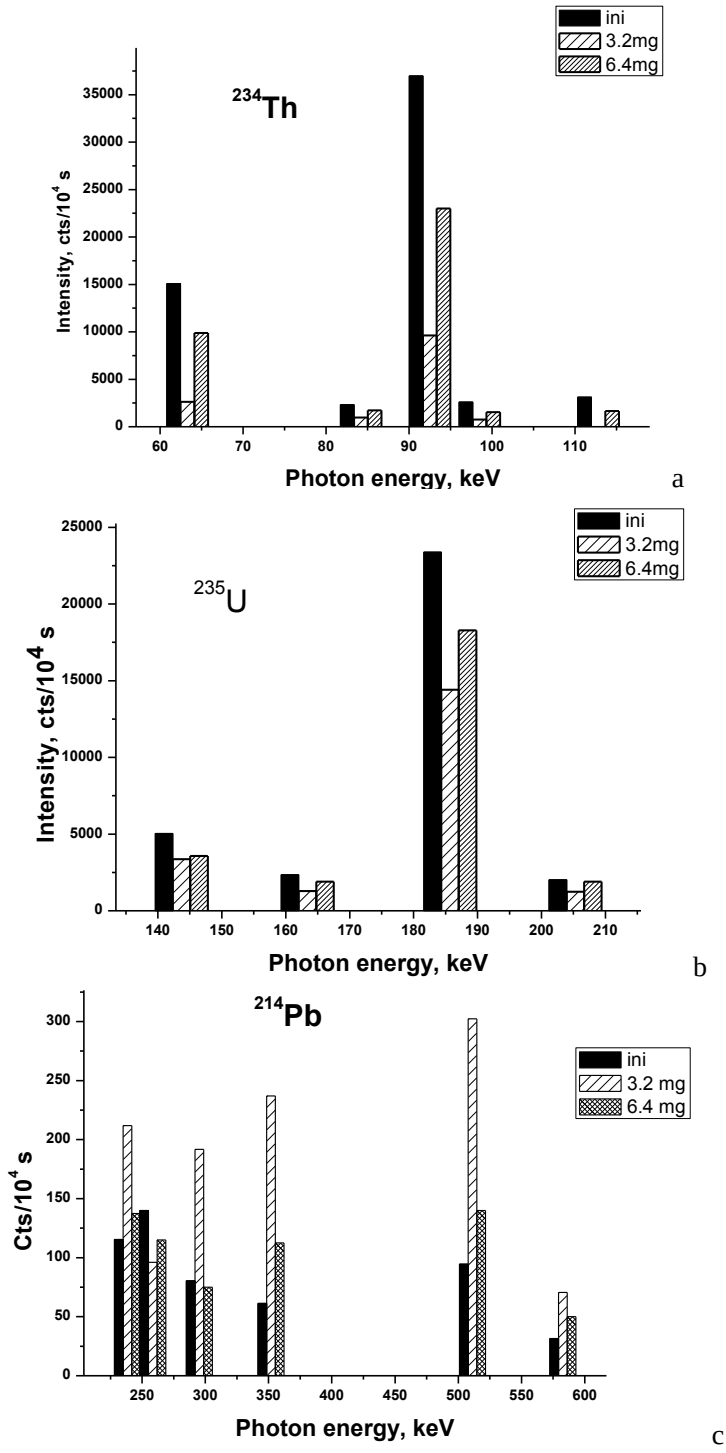

Figure 14. Activity change of ^{234}Th (a), ^{235}U (b), and ^{214}Pb (c) for two values of concentration of $UO_2(NO_3)_2$ in H_2O (3.2 and 6.4 mg/ml) after exposure to the third harmonics of a Nd:YAG laser at estimated peak power of 10^{12} W/cm^2. The most intense peaks of each nuclide are shown. 1 hour exposure at repetition rate of 10 Hz. Activities of nuclides in the non-exposed solution are labeled as INI. Gamma-measurements were carried out 11 days after laser exposure.

Plasmon resonance of Ag NPs is closer to 355 nm than that of Au NPs. Moreover, Ag NPs and NS is one of the most popular nano-objects that demonstrate the effect of Surface Enhanced Raman Scattering (SERS). Ag nano-entities demonstrate highest amplification of the light waves, and one may expect that their influence on the activity of radio-nuclides will be especially pronounced.

Laser ablation of a bulk Ag target in an aqueous medium containing Cl- ions, e.g., UO_2Cl_2, is accompanied by formation of AgCl compound instead of metallic species. For this reason laser exposure of Ag target was carried out in an aqueous solution of $UO_2(NO_3)_2$. The target was exposed to laser radiation at two values of salt concentration. The resulting change of activities is shown in Figure 14 [30].

The presented diagrams show that the activity of Thorium-234 is reduced by a factor of 3 at lower concentration of Uranil and to lesser extent at high concentration. The dependence of deviation of activity on the concentration of Uranil-chloride is typical for exposure to UV laser radiation. This radiation is absorbed by the Uranil-ion itself. The absorption of laser radiation leads to reduction of energy fluence on the target and, consequently, to lower concentration of Ag NPs.

The activity of Uranium-235 also decreases after laser exposure unlike the case of Au and Pd NPs. The increase of activity of ^{214}Pb in exposed solutions is of special interest. This nuclide stands at the end of ^{238}U branching. Its half-life is around 26 minutes (see Real-time gamma-emission section below). Figure 15 shows the fragment of gamma-spectrum of the solution in the vicinity of several peaks. One can see that their intensity in laser-exposed sample is much higher than in the initial one. Its increased activity 11 days after laser exposure indicates strong deviation from equilibrium of its parent nuclides. ^{226}Ra is the closest long-living nuclide to ^{214}Pb.

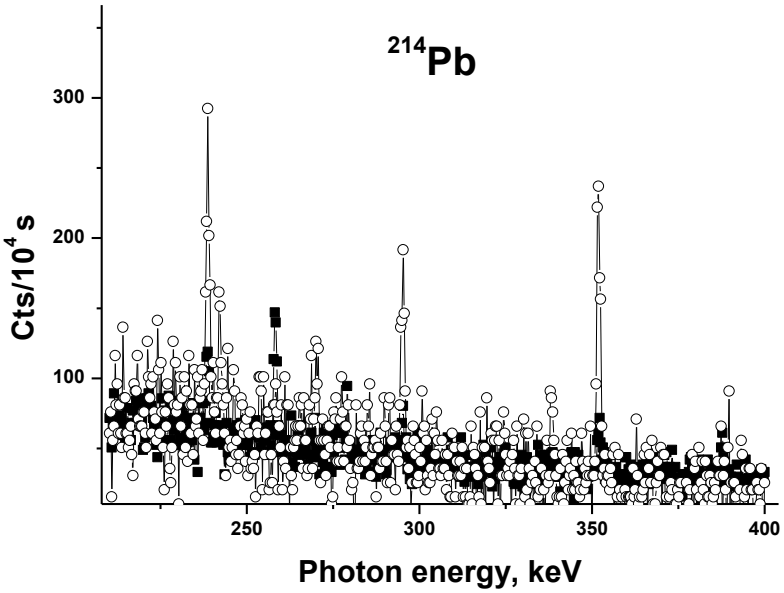

Figure 15. Fragment of gamma-spectrum with peaks of ^{214}Pb. Exposed solution (open circles), initial solution (solid squares). $UO_2(NO_3)_2$ concentration in H_2O of 3.2 mg/ml.

In turn, ^{226}Ra is the daughter nuclide to another long-living nuclide ^{234}U. Therefore, laser exposure causes strong deviation of equilibrium in the whole ^{238}U branching.

The increase of ^{214}Pb activity in solutions exposed to laser radiation is in good agreement with the results on non-equilibrium gamma-emission of Uranil solutions detected in real time during laser exposure (see below).

REAL TIME GAMMA-ACTIVITY OF SOLUTIONS UNDER LASER EXPOSURE

Similarly to laser exposure of aqua-ions of Thorium [26], laser exposure of aqueous solutions of Uranil-chloride is accompanied by non-equilibrium emission of gamma-photons. This section gathers the results on gamma-emission of solutions of Uranil in real time, during the laser exposure. Gamma-emission from samples under their irradiation with a Cu vapor laser was recorded in real time using a scintillation NaI gamma-spectrometer that was fixed near the working cell. Since the initial level of gamma-emission is comparable with the natural gamma-background, both the spectrometer and the working cell were placed into a 5 cm thick lead housing. The laser beam was directed to the working cell through a small aperture in the housing. Acquisition of gamma-photons was carried out through the wall of glass cell with the solution. The energy resolution of the scintillation spectrometer was 3 keV per channel [31]. The samples were the solutions of UO_2Cl_2 of natural isotope composition either in H_2O or D_2O. The typical concentration of Uranium salt was 50 mg/ml (0.15 M/L). Prior to the laser exposure, 1 ml of this solution was mixed with 1 ml of the colloidal solution of Au nanoparticles (NPs) obtained by laser ablation of a bulk gold target in either in H_2O or D_2O [31]. The average size of Au NPs was about 20 nm at concentration of 10^{14}cm^{-3}. The cell with the solution was sealed during the laser exposure to avoid the evaporation of the liquid. The average stationary temperature of the liquid during the laser exposure did not exceed 45°C. Two laser sources were used, either a visible range Cu vapor laser (wavelength of 510.6 and 578.2 nm and pulse duration of 10 ns) and the third harmonics of a Nd:YAG laser (wavelength of 1064 nm and pulse duration of 350 ps). The estimated peak power in the solution was 6×10^{11} and 10^{12} W/cm^2, respectively. The results obtained with these two laser sources are virtually the same. In order to avoid possible influence of the power supply of a Cu vapor laser on the gamma-spectrometer, shutting down of laser radiation was performed using shutting down the laser beam itself keeping the power supply running. Also, the spectrometer was fed from autonomous battery.

The general view of gamma-spectrum of the solution under laser exposure is presented in Figure 16. The main feature of the spectrum is the peak at small energy of photons between 50 and 60 keV. One can also see several peaks that correspond to Thorium-234 and Uranum-235 (90-100 keV range) and single peak of Uranium-235 at 186 keV.

Low-energy gamma-spectrum of the solution under laser exposure shows strong maximum in the 54-57 keV (see Figure 17). The real-time variation of activity of both ^{234}Th and ^{235}U are close to zerowithin the accuracy of measurements. The signal rapidly decays after shutting the laser radiation, and 16 hours after the exposure the signal is at the level of background (Figure 18).

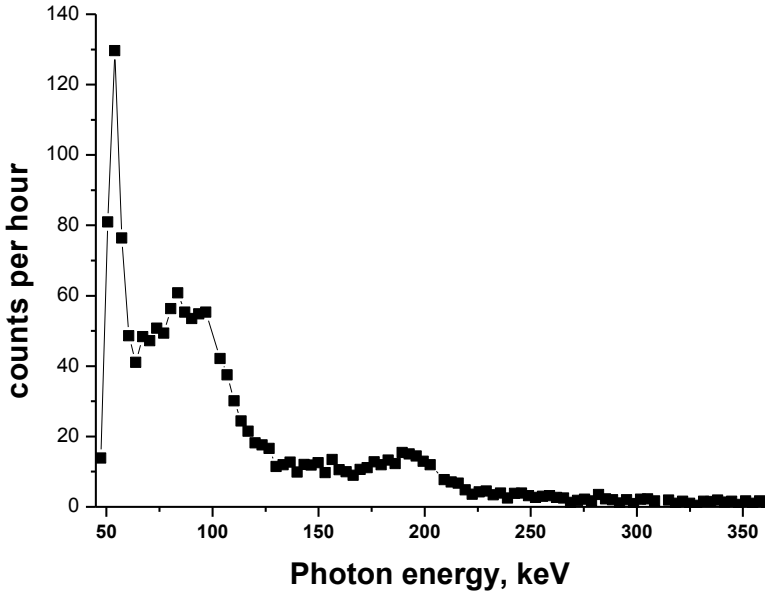

Figure 16. General view of gamma-spectrum of Uranil-chloride solution under exposure to radiation of a Cu vapor laser. Points are channels of the spectrometer.

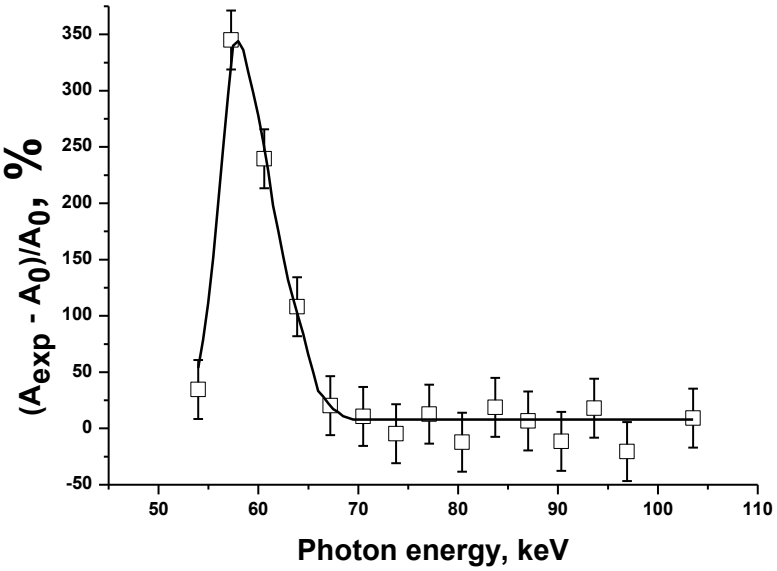

Figure 17. Normalized activity of the solution during laser exposure A_{exp} and before laser exposure A_0 in low-energy part of spectrum of the solution. Cu vapor laser, solution of UO_2Cl_2 in H_2O. Points are channels of the spectrometer.

The increase of gamma-activity in 50-60 keV is higher than before exposure by a factor of 3. The gamma-signal in this range increases under laser exposure during 1.5 – 2 hours and then reaches certain plateau value. The decay of this signal after shutting down the laser beam is shown in Figure 19. The activity rapidly decreases. Determination of the characteristic time of decay may stem the light on the nuclides that emit these gamma-photons.

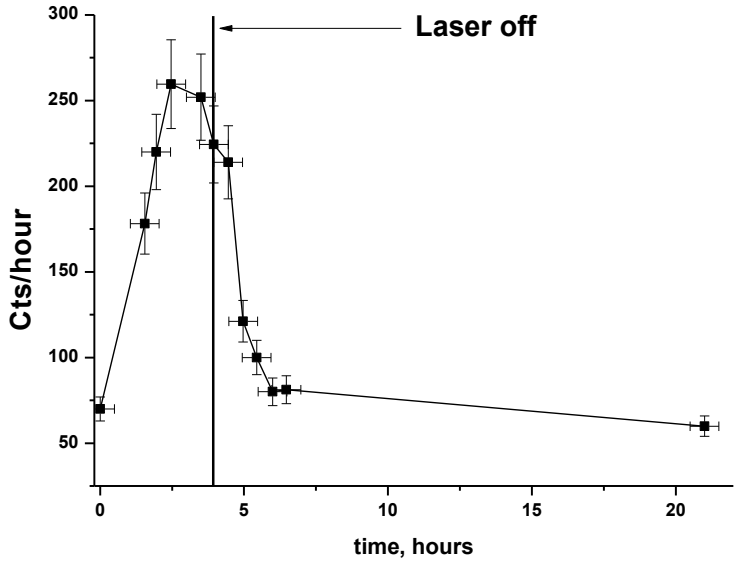

Figure 18. Kinetics of the gamma-emission of the solution of UO_2Cl_2 in D_2O with Au NPs at 53.4 keV photon energy. The acquisition time in each data point was 30 min. Cu vapor laser, the laser exposure starts at t = 0.

It was found that the time constants of decays at 54 and 57 keV are slightly different. This is illustrated in Figure 19, where these decays are plotted.

The decay of the gamma-emission is well approximated with exponential dependence with half- life of either 20 or 26 min with accuracy of ±3.5 min. According to reference data [33], this time constant is in good agreement with the half-life of the lead isotope ^{214}Pb of 26.8 min and bismuth isotope ^{214}Bi of 19.9 min.

These isotopes stand near the end of ^{238}U branching. Other lines of ^{214}Pb (at 241.9, 295.2, and 351.9 keV) are situated in the region of low sensitivity of the spectrometer used and cannot be detected with sufficient accuracy.

The activity of the samples at 54-57 keV reaches its maximum after the onset of the laser exposure (Figure 18). Apparently, this time is needed to produce sufficient amount of short-living isotopes of both Pb and Bi. However, the real-time variation of the gamma-activity of other isotopes, e.g., ^{235}U, ^{234}Th is small and lies within the accuracy of measurements of ±5%.

Cu vapor laser used in the experiments on real-time gamma-emission of Uranil-chloride solutions is relatively weak leaser source with its 10^{10} W/cm^2 intensity in the medium.

Exposure of solutions to radiation of this laser does not lead to any measurable changes in the activity of main nuclides presented in the solution, such as ^{235}U or ^{234}Th. That is why the change of activity in real time is observed only for short-living isotopes of lead and bismuth. However, the observed non-equilibrium gamma-emission confirms the presence of strong deviation from secular equilibrium in ^{238}U branching. The non-equilibrium gamma-emission of ^{214}Pb is in good agreement with results presented in previous sections on the increased activity of this isotope in Uranil-chloride solutions exposed to 150 picosecond laser radiation.

It is pertinent to note that the possibility to observe non-equilibrium gamma-emission of ^{214}Pb and ^{214}Bi is due to the local equilibrium between the rate of laser-induced generation of this isotope from its parent nuclides and laser-induced decay of these nuclides.

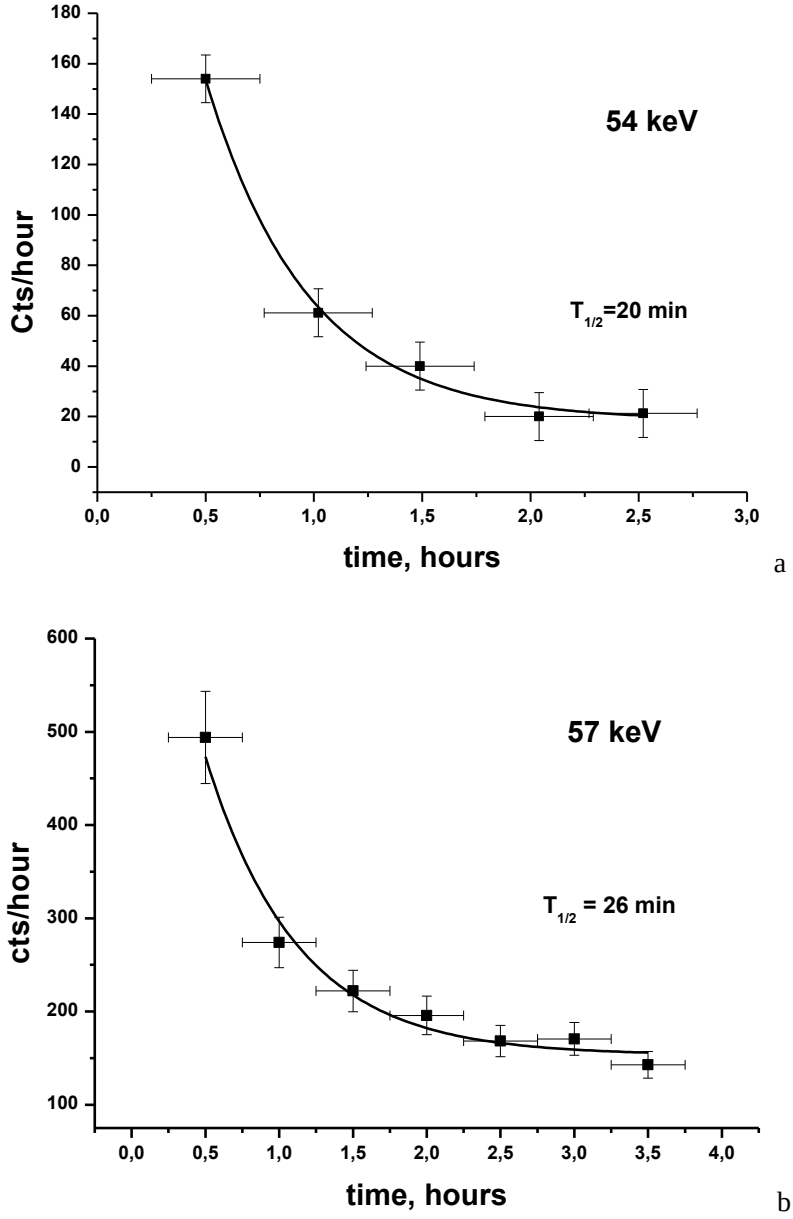

Figure 19. The decay of the gamma-emission at 54 keV (a) and at 57 keV (b) after the end of laser exposure. Exponential fit to the experimental points.

The effect of laser exposure on the activity of nuclides depends on the relative concentration of Uranium salt and metallic NPs.

The fraction of the latter should be sufficiently high to alter the activity of nuclides of Uranium branching. This is illustrated in Figure 20, where the normalized activities of various nuclides are plotted against the volume of the solution of UO_2Cl_2. One can see that the activity of both ^{214}Pb and ^{214}Bi increases after laser exposure by a factor of 20 at low concentration of Uranium salt [30].

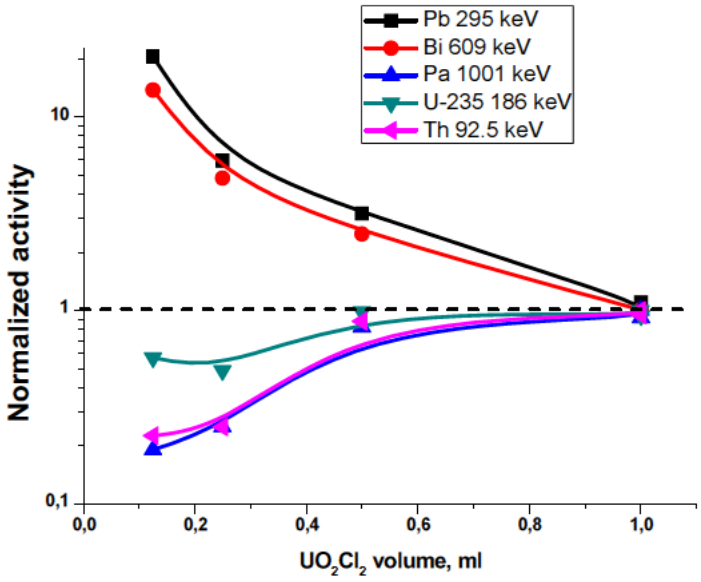

Figure 20. The activities of various nuclides normalized on their value in non-exposed solution as the function of the volume of UO_2Cl_2 solution in H_2O at concentration of 0.2 g/ml in the colloidal solution of Au NPs. Total volume of the solution is 2 ml, 1 hour exposure to the radiation of a Nd:YAG laser at 1064 nm at repetition rate of 10 kHz, pulse duration of 3 ns.

Other nuclides (^{234m}Pa, ^{235}U, ^{234}Th) demonstrate the decrease of activity after laser exposure, and this decrease is also highest at low concentration of Uranium salt. At high concentration of Uranium salt in the solution laser exposure causes only negligible changes of nuclide activities. This indicates that the effect of the laser field enhancement on nano-entities present in the solution plays a key role in laser initiation of nuclear decays.

LASER-INDUCED ACCELERATED DECAY OF ^{232}U

The conclusion on the variation of alpha-activity of ^{238}U under laser exposure was made on the basis of indirect measurements of gamma-activity of its daughter nuclides, ^{234}Th and ^{234m}Pa [28, 29]. The half-life time of alpha-decay of ^{238}U exceeds 10^9 years. It is expected that the influence of laser exposure on the alpha-activity will be more noticeable in case of a nuclide with shorter time of alpha-decay. ^{232}U may serve as such model nuclide. This is an artificial isotope with half-life of alpha-decay of 69 years. The sequence of decays of ^{232}U is as follows:

$$^{232}\mathrm{U} \xrightarrow{\alpha} {}^{228}\mathrm{Th} \xrightarrow{\alpha} {}^{224}\mathrm{Ra} \xrightarrow{\alpha} {}^{220}\mathrm{Rn} \xrightarrow{\alpha} {}^{216}\mathrm{Po} \xrightarrow{\alpha} {}^{212}\mathrm{Pb} \xrightarrow{\beta} {}^{212}\mathrm{Bi} \xrightarrow{\alpha} {}^{208}\mathrm{Tl} \xrightarrow{\beta} {}^{208}\mathrm{Pb}$$

This section describes the results of laser exposure of nanoparticles in aqueous solution of ^{232}U salt on its alpha-activity. The real-time gamma-emission of daughter nuclides ^{212}Pb and ^{208}Tl can be used for tracing the deviation from equilibrium under laser exposure [34].

The alpha-activity of the samples before and after laser exposure was measured using Ortec-65195-P alpha-spectrometer with accuracy of ± 5 %. Aqueous solution of $^{232}UO_2(NO_3)_2$ was divided into several parts. The first part with activity of 53.4 Bq/ml was used as the initial non-exposed solution.

This value of activity corresponds to 60 pg of ^{232}U per ml. Laser exposure of the solution was carried out by focusing the laser beam on a bulk gold target placed inside the solution with the help of an aspherical lens.

Initially the solution did not contain nanoparticles, the y were generated during the laser exposure of the target and dispersed in the solution due to convective motion. This scheme provides the constant level of nanoparticles density in the solution since they may agglomerate and sediment during laser exposure.

Four laser sources with different wavelengths and pulse duration were used for the exposure of solutions.

1. A Nd:YAG laser with wavelength of 1064 nm, pulse duration of 150 ps, estimated peak power in the solution of 10^{13} W/cm^2. Repetition rate was of 10 Hz, which corresponds to 3.6×10^4 laser pulses during 1 hour exposure.
2. The second harmonics of a Nd:YAG laser with wavelength of 532 nm, pulse duration of 150 ps, estimated peak power in the solution of 10^{12} W/cm^2. Repetition rate was of 10 Hz, which corresponds to 3.6×10^4 laser pulses during 1 hour exposure.
3. A copper vapor laser with wavelength of 510.6 nm, pulse width of 20 ns, estimated peak power in the medium of 10^{11} W/cm^2. Repetition rate of this laser was of 15 kHz, which corresponds to 2.16×10^9 pulses at 4 hour exposure.
4. A Nd:YAG laser with wavelength of 1064 nm, pulse duration of 350 ps, estimated peak power in the solution of 10^{12} W/cm^2. Repetition rate was of 300 Hz, which corresponds to 4.32×10^7 laser pulses during 4 hour exposure.

The laser sources have different pulse duration and wavelength of emission. The radiation of both copper vapor laser and the second harmonics of a Nd:YAG laser fits well the position of plasmon resonance of Au nanoparticles in water (around 530 nm).

Only approximate estimations of the peak power inside the solution with nanoparticles can be done. This is due to initiation of various non-linear effects inside the liquid at intensity level 10^{11} – 10^{13} W/cm^2 that may lead to defocusing of laser radiation. This can be, for example, the dynamic Kerr effect. On the contrary, self-focusing of the laser beam may lead to its filamentation and to the increase of laser intensity in the medium. Filamentation consists in the formation of several thin channels instead of the initial single beam due to dependence of the refractive index of medium on the laser intensity.

Finally, the presence of nanoparticles may alter the intensity level due to the absorption of laser radiation via plasmon resonance of charge carriers in nanoparticles or in the plasma produced around nanoparticles. Alpha-particles that are emitted by ^{232}U nuclei have higher energy than those emitted by ^{238}U. This is the reason of much shorter half-life of its alpha-decay.

Change of alpha-activity of the sample produced by exposure of a gold target in aqueous solution of ^{232}U salt in water to radiation of a copper vapor laser is accompanied by modification of gamma-activity of its daughter nuclides, such as ^{212}Pb and ^{208}Tl. This is illustrated by the following diagrams (Figure 21).

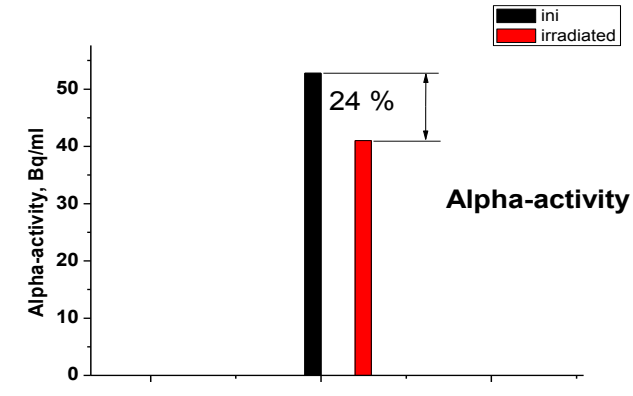

a

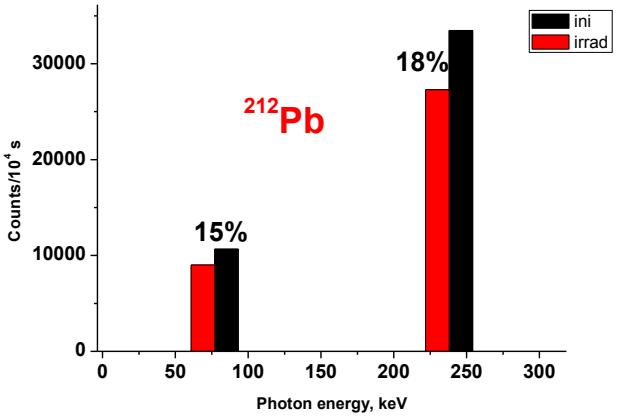

b

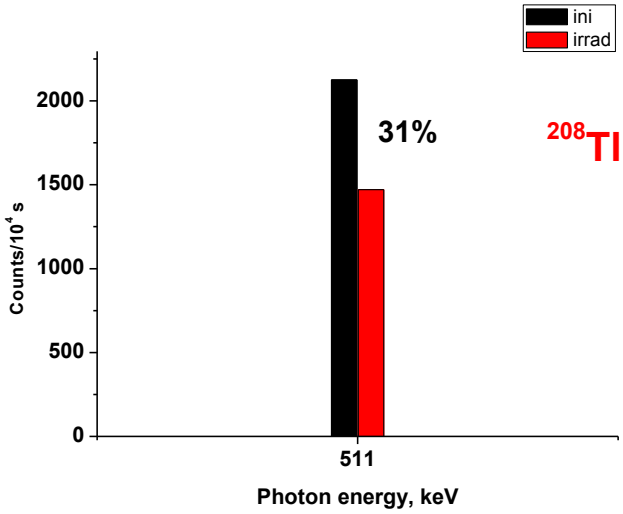

c

Figure 21. Change of alpha-activity of ^{232}U sample (a) and gamma-activities of ^{212}Pb (b) and ^{208}Tl (c) after exposure of a bulk gold target in aqueous solution of $^{232}UO_2(NO_3)_2$ to radiation of a Cu vapor laser during 4 hours (2.16×10^9 laser pulses).

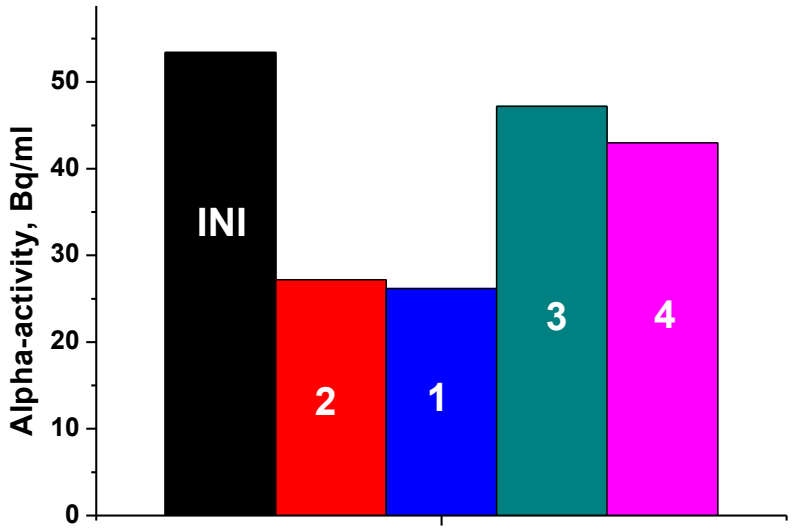

Figure 22. Diagram of comparison of relative effect of laser exposure on alpha-activity of the same solution to different laser sources. 1 and 2 corresponds to the second and first harmonics of a Nd:YAG laser with pulse duration of 150 ps, respectively. Column 3 indicates the alpha-activity of the solution after the exposure to radiation of a Cu vapor laser. Column 4 stands for the activity after exposure to the first harmonics of a Nd:YAG laser with pulse duration of 350 ps. Initial activity is designated by INI.

Similarly to laser exposure of ^{238}U salts, the final change of gamma-activity of daughter nuclides of ^{232}U may have different sign due to different rate of de-activation of gamma-activities of nuclides.

The effect of laser exposure sources is shown in Figure 22. One can see that the activity is decreased by a factor of 2 after 1 hour exposure to laser beam at intensity level of 10^{12} - 10^{13} W/cm^2. It is reasonable to suggest that the alpha-decay proceeds during the laser pulse, while the spontaneous decrease of alpha-activity during exposure is negligible.

This means that alpha-activity drops down by a factor of 2 during 5 μs, which is the total duration of all 150 ps laser pulses. In other words, the half-life of ^{232}U in the laser field is 5 μs instead of 69 years. About 10^{10} nuclei of ^{232}U decay during laser exposure. Another infrared laser radiation with pulse duration of 350 ps affects the alpha-activity of the solution to lesser extent despite to much higher number of laser pulses.

Finally, exposure of the solution of ^{232}U salt to radiation of a nanosecond Cu vapor laser produces quite small effect on the activity, though this effect is still higher than the accuracy of measurements. This relatively low effect is gained despite to much higher number of laser pulses absorbed in the solution (by a factor of 10^5) compared to a 150 ps laser source.

The above results one may conclude that the process of laser-induced alpha-decay has no threshold at least down to 10^{11} W/cm^2.

Laser-induced acceleration of alpha-decay can be observed not only with ^{232}U isotope. At low concentration of Uranil-chloride of ^{238}U (~ 10 mg/ml) laser exposure of its solution with Au NPs to radiation of a Nd:YAG laser with pulse duration of 3 ns during 1 hour at 10 kHz results in the decrease of alpha-activity of ^{238}U by a factor of 1.6. Gamma-activity of daughter nuclides of this isotope at this concentration is too weak for reliable measurements.

DEVIATION FROM SECULAR EQUILIBRIUM UNDER ELECTRO-EXPLOSION OF METALLIC FOILS IN SOLUTIONS OF URANIL SALT

Another example of influencing the secular equilibrium in the ^{238}U branching is the electro-explosion of metallic conductors in aqueous solutions of Uranil salts.

The experimental setup used in this series of experiments is completely different from the setup of laser-induced decays. However, the results are quite similar to what has been reported above on the laser-assisted acceleration of nuclear decays.

Electro-explosion of foils consists in discharge of a capacitor through a (thin) metal foil, either in air or in liquid. The electro-explosion of a metallic foil, e.g., Ti foil, immersed into the solution of Uranium salt in water also leads to significant deviation of activities of nuclides from their equilibrium levels. The experimental setup for foils electro-explosion was as follows [35]. Typical volume of aqueous $UO_2(NO_3)_2$ solution was of 20 ml. The battery of capacitances could store up to 22 kJ.

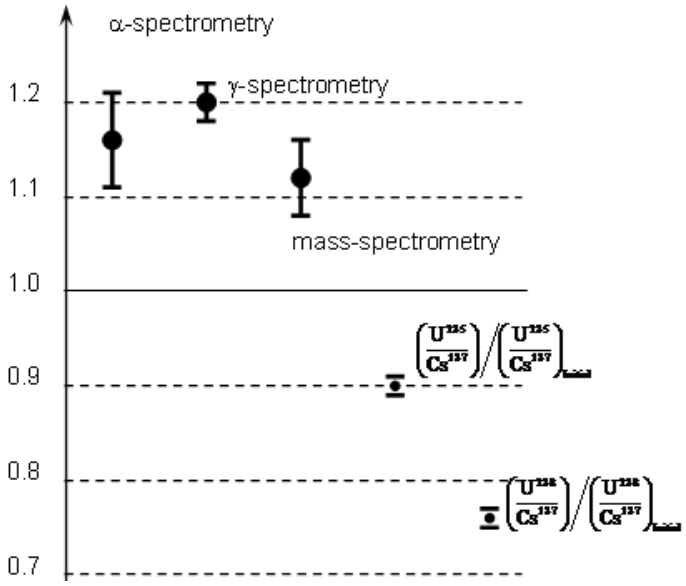

Figure 23. Ratio of activities $^{235}U/^{238U}$ after electro-explosion of a Ti foil in aqueous solution of $UO_2(NO_3)_2$ normalized on its value in the initial solution (courtesy of Prof. L.I. Urutskoev). ^{137}Cs was used as a label.

The stored energy at voltage of 4kV was discharged through a Ti foil placed into a sealed PMMA chamber. The peak value of current during the discharge was 120 kA, duration of the discharge was around 100 μs. After the discharge the metallic foil is dispersed into surrounding solution as molten micro- and nanoparticles of Titanium that interacts with water producing Ti hydroxides.

The deviation of equilibrium activity of nuclides of ^{238}U branching after electric discharge is illustrated in Figure 23. The authors also observed the restoration of ^{234}Th activity several months after the electric discharge. The perturbation of the equilibrium

between ^{234}Th and its daughter ^{234m}Pa nucleus detected by γ-spectrometry can be a result of the change in the β^--decay probabilities along different channels. This item was discussed in more detail previously [36].

Unlike the experiments on laser-induced decay described above, no noticeable excess over the background γ-radiation during the discharge was detected. This is probably due to the fact that electro-explosion of a foil is essentially single-pulse process. The discharge can be carried out only once, and then the chamber should be replaced for a new one.

The authors indicate that the ^{238}U concentration decreases more appreciably after the discharge than the ^{235}U concentration, and this is perceived as "effective" enrichment. The alpha-activity of ^{238}U demonstrates almost twofold decrease after the electric discharge. The authors also report the shift in the ratio of ^{238}U/^{137}Cs activity after electro-explsion of a Ti foil in aqueous solution of Uranil ion (see Fig. 23). In general, the shift of secular equilibrium observed under electro-explosion of metallic foils in Uranil solutions are qualitatively close to that observed under laser exposure of NPs in this solution.

POSSIBLE MECHANISMS OF LASER-INDUCED ACCELERATED DECAYS

As it follows from the above experimental data, the decay of ^{238}U under laser exposure of its solutions proceeds according to a classical sequence of alpha- and beta-decays of nuclides of its branching. However, the rate of this decay is many orders of magnitude higher than that of spontaneous decay (more than 10^9 years for ^{238}U). The sequence of nuclear transformations promoted via laser exposure of metallic NPs in aqueous solutions of Uranium salt do not deviate from their natural pathways, through natural sequence of decays of radio-nuclides, and the only parameter which is affected by laser radiation is the rate of the decays.

For any daughter nuclide of ^{238}U branching, e.g., ^{234}Th, the variation of its content in the probe can be written as a kinetic equation:

$$d[^{234}\text{Th}]/dt = [^{238}\text{U}]\exp(-t/t_{238\text{U}}) + k_1[^{238}\text{U}] - k_2[^{234}\text{Th}] - [^{234}\text{Th}]\exp(-t/t_{234\text{Th}}),$$

where $[^{23x}\text{N}]$ is the content of the corresponding nuclide, and at given volume of the solution is its concentration. In the conditions of secular equilibrium $k_1=k_2=0$, and the above equation describes the equilibrium activity of the corresponding nuclide. The increase of $[^{234}\text{Th}]$ is due to spontaneous alpha-decay of ^{238}U with half-life of $t_{238\text{U}}$ (negligible during the laser exposure) and laser-promoted alpha-decay of ^{238}U at rate constant of k_1. The decrease of $[^{234}\text{Th}]$ is due to the laser-promoted decay constant k_2 and its spontaneous decay with time constant of $t_{234\text{Th}}$ (also negligible). Since the duration of laser exposure is much shorter than the time of spontaneous decays mentioned above, the sign of the final variation of $[^{234}\text{Th}]$ is determined by the relative values of both k_1 and k_2. Experimental data allow concluding that the values of these constants is the function of experimental parameters, such as laser wavelength, laser peak power, the concentration of ^{238}U, etc. That is why the variation of $[^{234}\text{Th}]$ may have different sign after the laser exposure depending on the experimental parameters. For short-living isotopes of Uranium branching, such as ^{214}Pb and ^{214}Bi, their

spontaneous decay has to be taken into account, since their half-life is comparable with the duration of laser exposure.

It is known that alpha-decay proceeds via tunneling of alpha-particles through an energetic barrier, and the probability of tunneling is determined by its height E_b and width. Outside the nuclei the potential is self-consistent Colombian and is determined by the sum of electric fields of the nuclei and all electrons in the atom. The energy of laser photons is negligible compared with energy levels of nuclei, and direct excitation of nuclei energy levels is impossible. However, laser exposure of NPs may alter the configuration of the electric field outside the nuclei. The change of beta-decay time of nuclei under multiple ionization of the ^{187}Re atom has been reported [37]. Ionization of the atom alters the electric field around the nuclei and affects the life-time of its decay. Similar process may take place in case of laser exposure of metallic NPs in the solution that contains the nuclei of Uranium. This is due, first, to the high peak intensity of the laser radiation, which results in the high electric field E_{las} oscillating with optical frequency ω. Moreover, this field is enhanced due to the small size of nanoparticles, especially if the laser radiation is tuned into their plasmon resonance. Uranium atom (or aqua-ion in aqueous environment) in the vicinity of nanoparticle is subjected to high electric field of the laser wave E_{las}, and the barrier energy in this case E_{bexp} is modulated by the electric field of the laser wave: $E_{bexp} = E_b + E_{las}\exp(i\omega t)$. Since the probability of alpha-decay depends on E_b exponentially, even small variations of E_b can largely enhance it. Oscillations of alpha-particles inside the nuclei are several orders of magnitude higher, and therefore modulation of potential barrier induced by laser wave can be considered as quasi-stationary.

The mechanism of amplification of a weak Raman signal on either nano-protrusion of the metallic surface or on an isolated metallic nanoparticle is as follows [38]. Let us consider a particle (or protrusions) of radius R and dielectric function $\varepsilon_{met}(\omega)$. The flat incident monochromatic wave with field strength of E_0 can be written as follows:

$$E(r,t) = E_0 \exp(-i\omega t + i\vec{k}\vec{r})$$

In the electrostatic approximation the solution for the local field E_{loc} inside the particle is well-known:

$$E_{Loc}(\omega) = L(\omega)E_0 = \frac{3}{\varepsilon_{met}(\omega)+2}E_0$$

In a dielectric medium, the local factor L(w) is small if the light frequency is less than the bandgap value. However, for metals there is always an optical range in $-\varepsilon_{met}(\omega) < 0$. This means that the external field of certain frequency cannot penetrate inside the metallic sphere. In the resonant conditions , and the field strength at this frequency $E_{Loc}(\omega_{rec})$ is largely increased, while the absolute value remains finite. The precise calculations result in the following expression for the local factor:

$$\left|L(\omega_{rec})\right| = \frac{\left|\varepsilon'_{met}(\omega_{rec})\right|}{\varepsilon''_{met}(\omega_{rec})},$$

where $\varepsilon'_{met}(\omega_{rec})$ and $\varepsilon''_{met}(\omega_{rec})$ are the real and imageniary parts of dielectric function of a sphere at resonance frequency, respectively. For noble metals, such as Au or Ag, the absorption is small (ε''_{met}«1), and for Ag the local factor L(ω) may reach the value of 10-20. It is evident that the amplification occurs not only on the nano-entity itself but also in its vicinity.

In case of Raman scattering, both fields are amplified by the metallic objects, the incident light wave and the scattered Stokes signal, since their frequencies are very close to each other. As the results, the amplified Raman signal is proportional to $L^4(\omega)$ can be 10^5-10^6 times higher than out of resonance. The amplification of the incident wave is of order of $L^2(\omega)$.

The amplification factor G decreases with the distance from the particle as $G\sim (r_o/R)^{1/2}$, where r_0 stands for the characteristic size of nano-entity. This means that the field enhancement of the incident laser wave should still be significant at some distance from nano-structure.

According to known literature data, the field enhancement on NPs can be as high as 10^4 - 10^5. This gives the effective peak intensity near the nanoparticle of $I \sim 10^{17} – 10^{18}$ W/cm^2. The electric field that corresponds to this intensity is already comparable with internal atomic fields. Therefore, the electronic shell is largely perturbated. The advantage of laser exposure of NPs is that this field is gained inside the solution in their vicinity, otherwise a laser beam of this intensity can propagate neither in liquids nor in air due to various non-linear processes it induces in these media. High electrical field oscillating at laser frequency may alter both the height and the width of energetic barrier for alpha-particles that facilitates their tunneling and the accelerated alpha-decay of Uranium nuclei, either of ^{238}U or ^{232}U. The half-life time of the latter is only 69 yrs compared to 10^9yrs for ^{238}U. Therefore, the potential barrier for alpha-particles in ^{232}U nuclei is lower, and laser exposure of metallic NPs in aqueous solutions of this nuclide results in more pronounced effect. The same oscillating electric field causes the accelerated decay of both ^{234}Th and ^{234m}Pa nuclei through promotion of their beta-decay. The influence of laser exposure on the rate of beta-decay is higher than that on alpha-decay at otherwise equal conditions.

Estimations show that the alpha-decay of 10^6 nuclei of ^{238}U is promoted during one laser shot of 150 ps duration in the exposure conditions shown in Figure 9. The total number of alpha-decays of ^{238}U during the laser exposure is of order of 10^{10}, which represents roughly to 10^{-10} fraction of the total number of Uranium nuclei in the exposed solution. This is much below the accuracy of measurements of the alpha-activity of ^{238}U, which is typically ± 5%.

The enhancement of the electric field near the bulk target subjected to laser exposure can also be due to the presence of nanostructures on the gold target generated by short laser pulses of picosecond range of duration similar to that shown in Figure 5. The enhancement factor of 10^4 in SERS experiments has been realized in case of Au target nanostructured with picosecond laser pulses [39].

The selectivity of the laser-induced alpha-decay of ^{235}U and ^{238}U isotopes is not clearly understood at this moment. One might suggest that the frequency of oscillations of electronic shells around the nuclei is different for these two isotopes, so that the oscillating laser field is

far from resonance frequency for one isotope and closer to the other. This point requires further studies.

The highest deviations from equilibrium values of activities of ^{234}Th and ^{234m}Pa are observed under laser exposure of a bulk Au target in aqueous solution of UO_2Cl_2. This scheme is characterized by high concentration of Au NPs inside the laser beam. It is known that the nanoparticles generated by subsequent laser shots are then homogeneously distributed inside the working liquid. Let us estimate the concentration of NPs inside the laser beam n_b before the NPs leave it. The concentration of NPs in the whole volume of the cell V is n, and it was generated with N laser shots. Let us introduce the effective volume of the laser beam inside the colloidal solution, V_b. Then the following relation should be valid: $V_b n_b = nV$, and one can easily obtain:

$$n_b = nV/V_b.$$

The ratio V/V_b depends on the geometry of the particular experiment, and in typical conditions is of order of 10^{-4}, which means that the focused laser beam occupies only a small fraction of the volume of solution [40]. Therefore, the concentration of NPs inside the laser beam is by factor of 10^4 higher than the concentration of NPs in the bulk of the solution. The scheme of laser exposure of a metallic target in the aqueous solution of radio-nuclides (Figure 15) has a mere advantage over the laser exposure of the mixture of the colloidal solutions of NPs with the solution of radionuclides. Indeed, in that scheme the amplification of the laser field takes place both on NPs in the vicinity of the metallic target and on NS left on the target by previous laser pulse. Also, dense ensemble of NPs similar to that shown in Figure 1 or in Figure 2 can contain so called "hot points" that is closely placed nano-protrusions. These hot points can lead to the amplification of the light wave by a factor 10^{16} [41], which do not seem completely credible.

The most probable reason of the laser-assisted accelerated decays in nuclei is large perturbation of the electronic shells that surround Uranium nuclei. Let us estimate typical values of both the electric and magnetic field of the laser wave inside the liquid taking into account the amplification of both fields on metallic nano-entities, either NPs or NS.

At typical peak power of laser radiation in the medium of 10^{12} W/cm^2, amplification factor on either NPs or Ns is of order of 10^4, which is a moderate estimation. The electric field of the electromagnetic wave can be expressed as follows:

$$E(t) = E_0 \cos(\omega t) = \frac{1}{2} E_0 \left[\exp(i\omega t) + \exp(-i\omega t)\right]$$

In case of linear polarization of the radiation, the electric field in V/m can be expressed through its intensity in W/m^2 as follows:

$$E_0 = 27\sqrt{I}$$

For laser intensity I ~ 10^{16} W/m^2 the corresponding electric field E_0 ~ 10^{11} V/m, which exceeds the internal electric field. The corresponding magnetic field of the laser wave can be estimated as 4× 10^4 G.

High electric field can produce large perturbations in the electronic sub-system and alter the potential barrier for the tunneling of alpha-particles from ^{238}U nuclei. Also, the electric field of the laser radiation amplified on nano-entities may significantly increase the rate of beta-decays for nuclei in which they are permitted. This possibility is clearly seen from the experimental results presented above.

The possibility of excitation of nuclear levels of energy via generation of high-energy particles, similar to the experiments on laser ablation of targets in vacuum for laser exposure in liquids seems improbable. Indeed, despite to high values of electric field gained in the vicinity of nano-entities presented in the solution, the mean free path of particles in the condensed medium is too short to acquire the necessary energy.

Strong dependence of the acceleration of alpha-decay on the peak power of laser radiation in the medium should be related to the strength of fields of the laser wave. The natural measure of the electrical field is its value inside the atom or ion. The electric field of laser wave becomes comparable with inter-atomic field at intensity level of 10^{16} W/cm^2. Possible mechanism of laser-induced acceleration of alpha-decay can be illustrated as follows (Figure 24). Exposure of NPs to laser radiation leads to its amplification in the vicinity of NPs. If an ion of Uranil is situated near the exposed nanoparticle, then strong electric field of the laser wave disturbes its electronic shells. This perturbation causes the oscillations of the potential near its equilibrium value with the frequency of laser radiation. So do the width and the hieght of the potential barrier for tunneling alpha-particle.

Since the probability of tunelling depends on the barrier widt in an exponential way, so even its small variations can noticeably increase the rate of alpha-decay.

Owing to high concentration of NPs, the reduction of the width of potential barrier occurs near numerous NPs that are inside the focused laser beam. Also, the effect of laser-induced alpha-decay requires numerous laser pulses and has no apparent threshold down to intensities as low as 10^{10} W/cm^2.

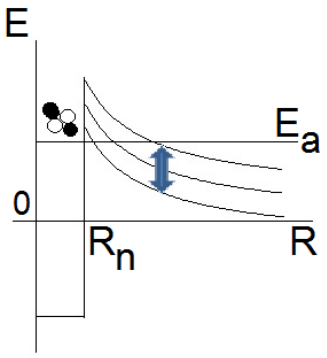

Figure 24. Qualitative illustration of the possible mechanism of laser-induced acceleration of alpha-decay. Open and closed circles symbolize protons and neutrons of the alpha-particle. E_a stands for the energy of tunneling alpha-particle, R_n is the radius of nuclei.

As it has been demonstrated above, the deviation of secular equilibrium in ^{238}U branching occurs in very different experimental conditions, such as laser exposure of NPs in the solution of Uranil-chloride and electro-explosion of a Ti foil in this solution. The common point between these two experimental setups is strong electric and magnetic fields generated in the solution of Uranium salt. It is known that high-current electric explosion of metal wires in a liquid induces strong magnetic fields ($H \sim 1$ MG) and high pulse pressures ($p \sim 10^5$ atm) [42].

The main parameter that is responsible for the deviation from secular equilibrium in experiments with electro-explosion is the magnetic field generated in the solution during the discharge through the foil.

Strong magnetic field changes the energy of the atomic electron shell and, hence, changes also the energy of any nuclear decay, as the decay energy is equal to the difference between the total energies of the initial and final systems with allowance for ionization energies of atoms or ions. For α-decay, the presence of strong magnetic field results in the increase in the decay energy and, hence, in the increase in the α-decay probability [43]. Since the ^{238}U α-decay energy is lower than the energies of the principal channels of ^{235}U α-decay, then the effect of the discharge on the alpha-decay of ^{238}U should be more pronounced. Also, the magnetic field changes the geometry of the problem: the spherical symmetry is replaced by the preferential direction along the magnetic field. This may by be considered as possible explanation of the selectivity of the deviation observed both in laser experiments and in experiments with the electro-explosion of foils in the Uranil solution. One more possible mechanism for $^{238}U/^{235}U$ selectivity is the parity of initial and final states of corresponding nuclei during alpha-decay, which is different for these two isotopes.

Theoretical investigations show that strong magnetic field can significantly accelerate permitted beta-decays [44] and can make possible forbidden beta-decays [45, 46]. Splitting of electronic energy levels in the magnetic field create new states to which the beta-decay becomes probable.

The difference between laser-induced decay and decay induced by electro-explosion is that measurable deviations of activities of nuclides can be observed after only one passage of current through a foil immersed into solution. This indicates that the Uranium nuclei are affected in the whole vessel containing the solution and not only in the microscopic area around the foil. The estimations presented above show that the magnetic field that is generated during the passage of the current through the foil is several orders of magnitude higher than that of the laser wave. The presence of sufficiently strong electric field during electro-explosion of the foil in Uranil solution seems doubtful. Indeed, the electric field may appear at the moment when the metallic foil is broken into pieces. However, the value of applied potential is unknown, since at this moment the battery of capacitors is partially discharged. Also, this field is applied locally just between the isolated pieces of Ti foil and cannot account for the equilibrium shift in the whole solution.

Laser action on the solution mediated by metallic NPs is essentially multi-pulse process. Lower value of both electric and magnetic fields compared to electro-explosion is compensated by the number of laser shots, which is typically of 10^3-10^4. Up to 10^7nanoparticles are inside the laser beam at each laser pulse, and this high number of active sites increases the efficiency of nuclear decays. The increased gamma-activity of Uranil solutions under laser exposure are observed due to accumulation of ^{214}Pb during exposure. No

accumulation is possible in case of electro-explosion of foils, since the duration of current is too short.

CONCLUSION

Thus, it is demonstrated that exposure of aqueous solutions of Uranil ions with metallic nanoparticles to laser radiation at peak intensity of 10^{12}-10^{13} W/cm^2 leads to significant shift of secular equilibrium in the activity of ^{238}U, ^{235}U, and ^{232}U and their daughter nuclides. Laser exposure of the solutions is accompanied by non-equilibrium gamma-emission assigned to the accumulation of ^{214}Pb and ^{214}Bi during laser exposure. Laser influence on the activity of nuclides has no apparent threshold on laser intensity at least down to 10^{10} W/cm^2.

Both approaches, laser exposure of Uranil solution with nanoparticles, and electro-explosion of metallic foils in this solution, lead to qualitatively similar results. The activity of nuclides of ^{238}U branching and that of ^{235}U undergoes irreversible change. Apparently, there is no need to explain this change addressing to unknown physical phenomena. Both setups are characterized by generation of intense electromagnetic fields in the solution that causes the distortion of electronic shells of Uranil ion. This, in turn, alters the probability of nuclear decays.

In both cases, neither fission products nor neutrons generation is detected. From practical point of view it is important that the decay of Uranium and its daughter nuclides can be accelerated with the use of commercially available laser and not only with unique laser systems. These commercial laser sources have high repetition rate of laser pulses, which allows accelerating the decay of radionuclides in reasonably short time. The presented results show that these lasers are efficient tools for acceleration of decay of heavy Uranium nuclei. The efficiency of laser-based technique for lighter nuclei remains to be explored for deactivation of nuclear waste.

ACKNOWLEDGMENTS

I thank my colleagues A.V. Simakin, L.I. Urutskoev, A. V. Goulynin, and A. A. Rukhadze for their help in experiments and useful discussions.

REFERENCES

[1] Wong, A. Grigoriu, J. Roslund, T.-S. Ho, and H. Rabitz, *Phys. Rev.* A84, 053429 (2011).

[2] Andreev A.V., Gordienko V.M., Dykhne A.M., Saveliev A.B., Tkalya E.V., 1997, *JETP Lett*. 66 (5) 312.

[3] Andreev A.V.; Volkov R.V.; Gordienko V.M.; Dykhne A.M.; Mikheev P.M.; Tkalya E.V.; Chutko O.V.; Shashkov A.A.; 1999, *JETP Lett*. 69 (5) 343.

[4] Schwoerer H., Gibbon P., Düsterer S., Behrens R., Ziener C., Reich C., Sauerbrey R. *Phys. Rev. Lett.*, 86 (11), 2317 (2001).

[5] V. S. Belyaev, A. P. Matafonov, V. I. Vinogradov, V. P. Krainov, V. S. Lisitsa, A. S. Roussetsky, G. N. Ignatyev, V. P. Andrianov, *Phys. Rev. E* 72 (2005), 026406.
[6] J. Nedersen, G. Chumanov, and T.M. Cotton, *Appl. Spectrosc*., (1993) *47*, 1959.
[7] M. S. Sibbald, G. Chumanov, and T.M. Cotton, *J. Phys. Chem*., (1996) *100*, 4672.
[8] Fojtik, A. Henglein, *Ber. Busenges. Phys. Chem*., (1993) *97*, 252.
[9] Henglein, *J. Phys. Chem*., (1993) *97*, 5457.
[10] M. Procházka, Štepánek, B. Vickova, I. Srnova, P. Maly, *J. Mol. Struct*. (1997) *410/411*, 213.
[11] M. Procházka, P. Mojzeš, J. Štepánek, B. Vléková, P.-Y. Turpin, *Anal. Chem*., (1997) *69*, 5103.
[12] M. Procházka, J. Štepánek, B. Vléková, I. Sronová, P. Malý, *J. Mol. Struc*., (1997) *410*, 213.
[13] Srnová, M. Procházka, B. Vléková, J. Štepánek, P. Malý, *Langmuir*, (1998) *14*, 4666.
[14] J.S. Jeon, C.H. Yeh, *J. Chin. Chem. Soc*., (1998) *45*, 721.
[15] M.-S. Yeh, Y.-S. Yang, Y.-P. Lee, H.-F. Lee, Y.-H. Yeh, and C.-S. Yeh, *J. Phys. Chem*., (1999) *B 103*, 6851.
[16] Takami, H. Kurita, and S. Koda, *J. Phys. Chem*., (1999) *B103*, 1226.
[17] S. Link, C. Burda, B. Nikoobakht, and M.A. El-Sayed, *J. Phys. Chem*., (2000) *B104*, 6152.
[18] F. Mafuné, J. Kohno, Y. Takeda, T. Kondow, H. Sawabe, *J. Phys. Chem*., (2000) *B 104*, 9111.
[19] F. Mafuné, J. Kohno, Y. Takeda, T. Kondow, H. Sawabe, *J. Phys. Chem*., (2001)*B 105*, 5114.
[20] A.V. Simakin, V.V. Voronov, G.A. Shafeev, R. Brayner, and F. Bozon-Verduraz, *Chem. Phys. Lett.*, (2001) *348*, 182.
[21] S.I. Dolgaev,A.V. Simakin, V.V. Voronov, G.A. Shafeev, F. Bozon-Verduraz, *Appl. Surf. Sci*., (2002) *186*, 546.
[22] P. V. Kamat, M. Flumiani, and G.V. Hartland, *J. Phys. Chem*., (1998) *B 102*, 3123.
[23] G.W. Yang, *Progress in Materials Science*, (2007) 52, 648–698.
[24] G.A. Shafeev, Formation of nanoparticles under laser ablation of solids in liquids, in: *Nanoparticles: New Research*, editor Simone Luca Lombardi, pp. 1 -37, 2008, Nova Science Publishers, Inc., New York
[25] E. V. Zavedeev, A. V. Petrovskaya, A. V. Simakin, G. A. Shafeev, *Quantum Electronics*36(10) (2006), 978-980.
[26] A.V. Simakin, G.A. Shafeev, arXiv:0906.4268; A.V. Simakin, G.A. Shafeev, *Physics of Wave Phenomena*, 16 (4) (2008) 268-274; A.V. Simakin, G.A. Shafeev, *Journal of Optoelectronics and Advanced Materials*, (2010) 12(3), 432 – 436.
[27] http://isotopes.lbl.gov/isotopes/isoexpl.html.
[28] A.V. Simakin, G.A. Shafeev, *Quantum Electronics* 41 (7) 614 – 618 (2011).
[29] A.V. Simakin, G.A. Shafeev, *Physics of Wave Phenomena* (2011) 19(1), 30–38.
[30] G.A. Shafeev, *Applications of Nd:YAG Lasers: From Nano-Structures to Nuclei*, 2011, an open access book at www.novapublishers.com.
[31] Alexandr V. Simakin and Georgy A. Shafeev, *Journal of Materials Science and Engineering B* 1 (2011) 618-625.
[32] G.A. Shafeev, Laser-Based Formation of Nanoparticles, in: *Lasers in Chemistry*, Wiley VCH, Wienheim, 2008, pp. 713-741.

[33] http://nucleardata.nuclear.lu.se/nucleardata.
[34] A.V. Simakin, G.A. Shafeev, arxiv.org/abs/1112.6276 at www.arxiv.org.
[35] G. Volkovich, A. P. Govorun, et al., *Bull. ofLebedev Phys. Inst.* (2002) No 8, 45; *Ann. Fond. L. de Broglie*30 (2005) 63.
[36] F. Cardone, R. Mignani, and A. Petrucci, *Phys. Lett.* A 373 (2009) 1956.
[37] F. Bosch, T. Faestermann, J. Friese, F. Heine, P. Kienle, E. Wefers, K. Zeitelhack, K. Beckert, B. Franzke, O. Klepper, C. Kozhuharov, G. Menzel, R. Moshammer, F. Nolden, H. Reich, B. Schlitt, M. Steck, T. Stöhlker, T. Winkler, K. Takahashi, *Phys. Rev. Lett.* (1996) 77, 5190.
[38] O.A. Aktsipetrov, *Soros Educational Journal*, (2000), vol. 6.
[39] S. Lau Truong, G. Lévi, F. Bozon-Verduraz, A. V. Petrovskaya, A. V. Simakin, G. A. Shafeev, *Applied Surface Science* 254 (2007), 1236-1239.
[40] A.V. Simakin, V.V. Voronov, N.A. Kirichenko, and G.A. Shafeev, *Appl. Phys.*, A79(2004) 1127-1132; S. Lau Truong, G. Levi, F. Bozon-Verduraz, A. V. Petrovskaya, A. V. Simakin, G. A. Shafeev, *Appl. Phys*.A89(2) (2007), 373-376.
[41] SurbhiLal, Stephan Link, Naomi J. Halas, *Nature Photonics*, (2007) Vol. 1, No. 11. (01 November), 641-648.
[42] *Exploding wires* (Eds. W. G. Chace and H. K. Moore), Plenum Press, New York 1962; Y. Bakshaev et al., *Plasma Phys. Rep*. 27 (2001) 1039; A. Velikovich et al., *Phys. Plasmas* 14 (2007) 022706.
[43] L. I. Urutskoev and D. V. Filippov, *Physics-Uspekhi* 47 (2004) 1257.
[44] Philippov D.V., *Physics of Atomic Nuclei*, 70(2), 280–287 (2007).
[45] Philippov D.V., *Physics of Atomic Nuclei*, 70(12) 2068–2076 (2007).
[46] Yu.P. Gangrsky, F.F. Karpeshin, M.B. Trzhaskovskaya, Yu.E. Penionzhkevitch, *Physics of Atomic Nuclei*, 71(6), 979-983 (2008).